MASTERARBEIT

Titel der Masterarbeit

„Growth Factor-Induced Epithelioid-Sarcomatoid Transition in Malignant Pleural Mesothelioma Cells?"

verfasst von

Christina Wagner, BSc

angestrebter akademischer Grad

Master of Science (MSc)

Wien, 2015

Contents

1 Introduction

1.1 Malignant Mesothelioma

Malignant mesothelioma (MM) is a relatively rare form of cancer, which can affect the pleura (pleural mesothelioma), the peritoneum (peritoneal mesothelioma) and rarely the pericardium (pericardial mesothelioma) or the tunica vaginalis testis [1]. It derives from the mesothelium, a non-adhesive, protective surface which covers the internal organs and structures of the body. Mesothelial cells are involved in the transport of fluids, antigen presentation, inflammation and tissue repair. Although the mesothelium derives from the mesoderm and is not a typical epithelial tissue, it expresses epithelial, but also mesenchymal markers [2].
Mesothelioma is a highly aggressive tumor with a long period of latency (20-40 years), a poor prognosis and limited therapeutical options due to its diffuse growth and invasive abilities.

The most common form of MM is malignant pleural mesothelioma (MPM, 70-90%), followed by malignant peritoneal mesothelioma (10-30%). The median survival time of patients with MPM is 6 to 18 months, depending on the histological subtype (for the histological subtypes of MPM see subsection 1.1.2 on page 2) and the stage of the disease at diagnosis. MPM derives from the pleura (see figure 1) and usually spreads locally along it, though metastasis to other organs can occur in the later stages of the disease [3].
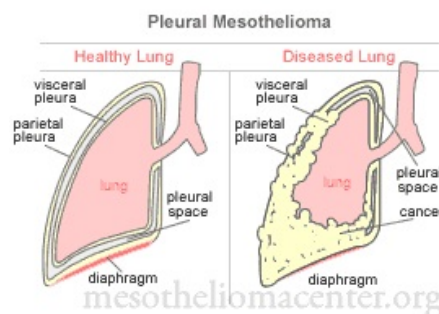

Figure 1: Pleural mesothelioma (www.mesotheliomacenter.org; 2014, Dec. 04).

1.1.1 Cause and Incidence

All of the three varieties of malignant mesothelioma are mainly a consequence of exposure to asbestos. Hence the highest annual incidence rates of about 30 cases per million correspond to industrialized countries with high asbestos use such as Australia, Belgium and Great Britain [4]. Although the use of asbestos in western countries stopped in the 1970s, a peak of incidence is expected around 2015, due to the long period of latency [1]. Since asbestos is still produced and used in some countries like Brazil, China, Russia and India, an increase in incidence and death of MM is expected there [5].
Erionite, another carcinogenic mineral fiber, is less widespread than asbestos but also associated with a number of MM cases. Also there are possible co-factors for the development of MM, such as radiation exposure, genetic predisposition and viral infection [6].

A perseverative exposure to asbestos increases the risk of developing malignant mesothelioma [4]. Asbestos fibers settled in the mesothelial tissue which are too long to be completely enclosed by macrophages can not be phagocytosed and therefore cause inflammation in the tissue [7]. Since the reactive macrophages present in the tissue secrete various mutagenic oxygen and nitrogen species, the chronic inflammation can result in carcinogenesis, due to alteration of the DNA of surrounding cells. Also other pro-inflammatory molecules such as HMGB-1 (High-mobility group protein B1) and TNF-α (tumor necrosis factor alpha) are released [6]. TNF-α induces NF-κB (nuclear factor kappa-light-chain-enhancer of activated B-cells) signaling, which was shown to induce carcinogenesis in an inflamed tissue in various cancer models, including mesothelioma [8].
In cultured cells exposed to asbestos DNA strand breaks occur, resulting in inheritable changes of the chromosomes. These changes can be be induced by physical interference of the asbestos fibers in the mitotic process. Frequent abnormalities in human mesotheliomas involve alterations in chromosomes 1, 2, 3, 6, 7, 9, 11, 17 and 22 [9].

1.1.2 Histological subtypes of MPM

There are three main histological subtypes of MPM: the sarcomatoid (7-20%), the epithelioid (50-70%) and the biphasic or mixed subtype (20-35%), see figure 2. Sarcomatiod and partially also the mixed MPM show a more or less distinct fibroblast-like, spindle-shaped morphology and a more aggressive behavior than the epithelioid MPM. The morphology of the epithelioid MPM resembles that of the normal pleura [10]. There are no accepted immunohistochemical markers for the different subtypes. Also it is unknown, what causes the different types, but the fibroblastoid morphology of the cells and the more aggressive behavior of sarcomatoid MPM suggest an epithelial to mesenchymal transition (EMT) in the tumor cells of sarcomatoid MPM [10].
Metastasis of MPM depends mainly on the histological subtype. In two thirds of

the cases with sarcomatoid subtype distant metastases occured, whereas in cases with epithelioid or biphasic subtype only one third of the patients had metastases [11]. Distant metastases of the sarcomatiod type can occur in the contralateral pleura and the lung, in intra- and extra-thoracic lymph nodes as well as in the liver, bone and brain. In cases with epithelioid tumors the mediastinal lymph nodes were affected more frequently [1, 11].

epithelioid (50-70%)   sarcomatoid (20-35%)   biphasic (7-20%)
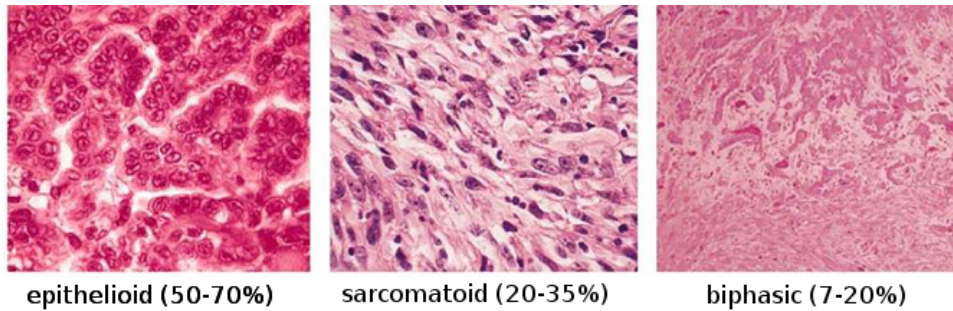
Figure 2: The three histological subtypes of MPM and their frequency of occurrence, image taken from Schelch 2011 [12].

1.1.3 Treatment of MPM

MPM is usually highly resistant to current chemo- and radiotherapy methods. None of the known approaches have proven curative, but some can at least prolong survival as well as ease the symptoms such as breathlessness and thoracic pain. A combination of cisplatin and pemetrexed, both cytostatic drugs, decreases the tumor burden. Because of the diffuse growth of the tumor along the pleura, radical radiotherapy is almost impossible without damaging other organs such as lung or heart. Therefore radiotherapy can only be delivered locally, as a part of a trimodality treatment discussed below [3, 12]. Another therapeutic approach is radical surgery, either a pleurectomy or an extrapleural pneumonectomy (EPP). A pleurectomy is performed in cases where the tumor only spreads superficially without invading other areas. EPP is performed in cases where the tumor already invades surrounding tissues or organs. This method includes removal of the pleura, the lung, the diaphragm and the pericardium, if affected [13]. Since EPP was associated with increased mortality and morbidity, the idea of aggressive surgery as the ultimate cure of the disease was discarded [14]. Besides, even after EPP, MPM can recur locally, and not all patients are suitable for this treatment because of an overall bad condition [3]. In the last 10 years, trimodality treatment was established as a preferential therapy [14].
Trimodality treatment includes surgery, followed by local radiotherapy to the thorax, to prevent local recurrence, and chemotherapy, to decrease the risk of metastases [1, 3]. In this multimodal approach patients who underwent a pleurectomy followed by radio- and chemotherapy showed a higher survival rate compared to patients with an EPP followed, if possible due to the patients condition, by radio- and/or chemotherapy [3]. Various trials showed, that trimodality treatment with

first induction chemotherapy with cisplatin and pemetrexed, followed by surgery and radiotherapy are also feasible and beneficial for the survival rate of selected patients, depending on the patient's overall fitness and the stage of the disease [15, 16, 17].

1.2 Fibroblast Growth Factors and their Receptors

Fibroblast growth factors (FGFs) and their receptors (FGFRs) form a cellular signaling-system, which plays an important role in many physiological processes such as embryonic development, cell proliferation and survival, migration, wound healing and angiogenesis. FGFs also contribute to the regulation of electrical excitability of cells and can also act as hormones that regulate metabolism [18, 19]. FGFRs and their ligands also have oncogenic features. Deregulation of FGF signaling mediates uncontrolled survival, proliferation, migration and blood vessel recruitment of tumor cells [20].

1.2.1 Fibroblast Growth Factors

The FGF family in vertebrates consists of 22 members, all of them are polypeptide mediators with an amino acid similarity of 13 to 71% and a molecular mass between 17 to 34 kDa [21]. Of these 22 FGFs, four (FGF11-14) are so called fibroblast homologous factors (FHFs), which carry a nucelar localisation signal and are not secreted (intracrine FGFs). Since they are not secreted, they also act FGFR-independent. The other 18 members of the family can be separated into two subgroups: the hormone like subgroup (FGF15/19 - note: FGF19 is the human orthologue of FGF15 in mice - FGF21 and 23; endocrine FGFs) and the canonical subgroup. This canonical subgroup can be further divided into 5 groups by means of their structural homologies and phylogeny [20, 22]:

- FGF1 group: FGF1, FGF2

- FGF4 group: FGF4, FGF5, FGF6

- FGF7 group: FGF3, FGF7, FGF10, FGF22

- FGF8 group: FGF8, FGF17, FGF18

- FGF9 group: FGF9, FGF16, FGF20

For a better overview of the families see also figure 3.

All of those FGFs except FGF1 and 2 are secreted via the endoplasmic reticulum due to their secretion signaling peptide. FGF1 and 2 lack this signal sequence and either utilize another secretion pathway or remain intracellular, only set free from decaying cells [20, 22]. The 18 ligands act through four highly conserved,

high affinity tyrosine kinase receptors, the fibroblast growth factor receptors 1-4. These receptors are transmembrane proteins with an intracellular tyrosine kinase domain, one single-pass transmembrane domain and an extracellular ligand binding domain (see also 1.2.2 on page 6) [20, 23].

The secreted FGFs bind to the heparan sulfate (HS) glucosaminoglycan side-chains of HS proteoglycans (HSPG) in the extracellular matrix (ECM), which limits their diffusion but prolongs their half-life through guarding the FGFs from heat, pH and proteolytic degradation [23]. The FGFs can be released from the HS through binding to specific FGF binding proteins (FGF-BP), which lowers the affinity to HS, or by the action of extracellular proteolytic enzymes such as heparitinases and proteases. This makes the FGFs available for signaling, for example shown for FGF1 and 2 during wound healing [24]. The free ligands can then bind to HS and the FGFR on the cell surface, forming a stable ternary complex necessary for the ligand-receptor interaction [19, 23]. Members of the endocrine FGF subfamily need a co-receptor in addition to the FGFR to carry out their metabolic control functions, namely proteins of the Klotho family [25].
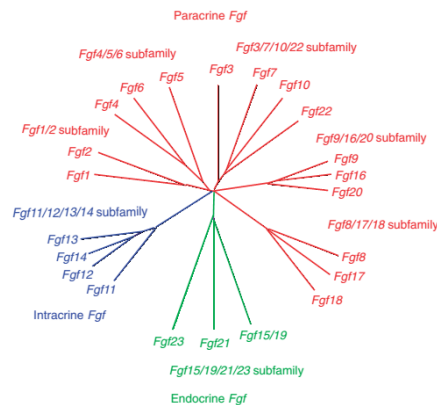
Figure 3: The FGF family, image taken from Itoh and Ornitz [18].

FGFs are important players throughout embryonic development, from gastrulation to organogenesis. Formation of the limbs, the nervous system and also of organs like heart and lungs depends on FGF signaling [20, 22]. During development, FGFs are often used for directional signaling between different tissue types via expression of specific receptors and FGFs, as described later on [21]. A tightly regulated epithelial-mesenchymal communication via FGFs is for example required during the induction of the mesoderm during early development. It was shown in mouse-models that FGF knock-out often leads to an embryonic lethal phenotype or to severe deficits in organogenesis, resulting in an early death of the mice [21, 22].

In the adult tissue, FGFs play an important role in tissue repair, wound healing and angiogenesis. Especially FGF2 is known to induce the sprouting of new vessels during these processes [22].

1.2.2 Fibroblast Growth Factor Receptors and Signaling Pathways

As mentioned before, there are four FGF receptors. These receptors consist of an extracellular ligand binding domain with three immunglobulin-like domains (Ig-like domains I-III), a single-pass transmembrane domain and an intracellular tyrosine kinase domain. The FGFRs belong to the family of receptor tyrosine kinases, a group of transmembrane receptors sharing structural and functional homologies [20, 22]. Four genes encode the FGFRs, through alternative splicing the 7 main isoforms are formed. FGFR1-3 each have IIIb and IIIc isoforms, created through alternative splicing of the Ig-like domain III. FGFR4 has no IIIb isoform. Since the Ig-like domains II and III alone are needed to mediate ligand-binding, alteration of these domains influences the ligand binding specificity (for an overview of the receptor isoforms and their ligands see table 1) [26]. It was found, that the alternative splicing is tissue specific. The FGFR IIIc isoforms are mainly expressed in mesenchymal cells, whereas the FGFR IIIb isoforms are predominantly expressed in epithelial cells. This enables directional signaling between the two tissues via expression of ligands stimulating the corresponding receptor on the other cell type [20, 21]. Through this mechanism, also autocrine stimulation of the cells is prevented or at least limited [21].

In the region between domain I and II lies the so called acid box, an acidic, serine-rich region which is specific for FGFRs. This region, together with the Ig-like domain I, plays no role in ligand binding but is proposed to be involved in receptor autoinibition [20, 26].

Table 1: FGFRs and their ligands, table taken from Heinzle et al. [22]

Receptor	Ligands
FGFR1 IIIb	FGF1, FGF2, FGF3, FGF10, FGF22
FGFR1 IIIc	FGF1, FGF2, FGF4, FGF5, FGF6, FGF8, FGF9, FGF16, FGF17, FGF18, FGF20, FGF21, FGF23
FGFR2 IIIb	FGF1, FGF3, FGF7, FGF10, FGF22
FGFR2 IIIc	FGF1, FGF2, FGF4, FGF5, FGF6, FGF8, FGF9, FGF16, FGF17, FGF18, FGF20, FGF21, FGF23
FGFR3 IIIb	FGF1, FGF9, FGF16
FGFR3 IIIc	FGF1, FGF2, FGF4, FGF5, FGF6, FGF8, FGF9, FGF16, FGF17, FGF18, FGF20, FGF21
FGFR4	FGF1, FGF2, FGF4, FGF5, FGF6, FGF8, FGF9, FGF16, FGF17, FGF18, FGF19, FGF20, FGF21, FGF23

The signal from the ligands is transported from the receptors to various effector proteins and transcription factors in the nucleus through a complex system of phosphorylation, dephosphorylation and exchange of GTP/GDP, executed by various adaptor and scaffolding proteins, kinases, phosphatases and nucleotide

exchange proteins [27, 28].

Upon ligand binding to the receptor, the FGFRs dimerize and become active. The cytoplasmic kinase domains trans/autophosphorylate each other on various tyrosine residues, and the phosphorylated residues serve as docking sites for various adaptor proteins needed for downstream signaling, for example FRS2 (FGFR substrate 2) and PLC-γ (Phospholipase C-γ) (see also figure 4) [20, 23]. FRS2 is an adaptor protein which binds to the juxtamembrane region of the receptor via its phosphotyrosine-binding domains (PTB), where it links several pathways to an active FGFR [19, 20]. When the receptor is activated, FRS2 becomes phosphorylated itself on several tyrosine residues and acts as docking site for other adaptor proteins, such as Grb2 (Growth factor receptor bound protein 2). Grb2 binds to the phosphorylated FRS2, where it recruits GAB1 (Grb2-associated binding protein 1) as well as SOS (son of sevenless) [20, 23].

SOS is a guanine nucleotide-releasing factor for Ras, a small GTP-binding protein, which is activated through exchange of GDP with GTP. The active Ras recruits Raf to the plasma membrane and activates it via interaction with the N-terminal regulatory domain of Raf. This interaction leads to dephosphorylation of negative regulatory sites and conformational changes in Raf, which lead to exposure of the kinase domain and to subsequent phosphorylation of various residues at activating sites (e.g Ser338 and Tyr341) [29]. Raf then phosphorylates MEK1 (mitogen activated protein kinase 1), a tyrosine and serine/threonine dual-specifity protein kinase, which in turn activates ERK1 and 2 (extracellular signal regulated kinases 1 and 2). ERKs are serine/threonine kinases with over 600 substrates, including transcription factors for growth factors and cytokines. This pathway mostly transmits proliferation signals [20, 27, 28]. Note that there are 4 different Ras proteins (Ha-Ras, N-Ras, Ki-Ras 4A and 4B) as well as 3 Raf proteins (A-Raf, B-Raf and Raf-1), which differ in their ability to activate the downsream pathways [27].

The scaffolding protein GAB1 recruits PI3K (phosphoinositide-3-kinase), which in turn activates the serine/threonine kinase Akt (also known as protein kinase B (PKB). Signaling via this pathway stimulates the expression of anti-apoptotic proteins, therefore promoting survival of the cells [20, 30].

Independent of FRS2, PLC-γ can bind to a phosphorylated tyrosine near the carboxyl terminus of the receptor via its SH2 (Src homology 2) domain. The active PLC-γ hydrolyses phosphatidylinositol-4,5-biphosphate (PIP2) to two second messengers phosphatidylinositol-3,4,5-triphosphate (PIP3) and diacylglycerol (DAG), the latter activating PKC (protein kinase C), which can also phosphorylate Raf [19, 30].

Also other pathways not further described here can be activated by FGFRs, among them the STAT (signal transducer and activator of transcription) signaling pathway [19].
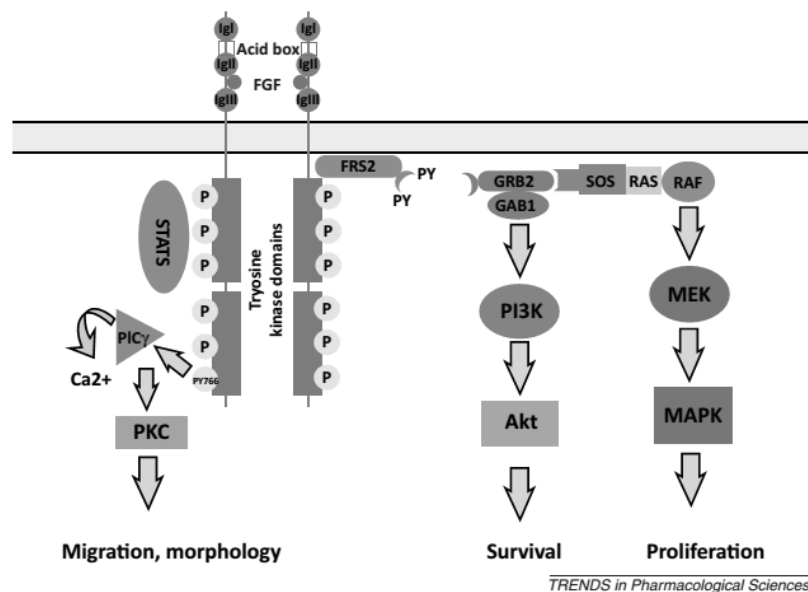
Figure 4: Components of the downstream signaling pathways, image taken from Liang et al. [31].

Signaling via the FGFRs and their downstream pathways can be attenuated through several mechanisms. Auto-regulatory feedback-loops, induced through the FGFR signaling itself, control the duration and the intensity of the signal. The receptors can be internalized and degraded or recycled, either via ubiquitination or endocytosis [20, 22]. Ubiquitination of the FGFRs is carried out by the ubiquitin ligase Cb1, which can bind to active FRS2 and mediate the ubiquitination of the receptor. The extent of ubiquitination differs between the four FGFRs, which seems to influence the efficacy of the degradation of the receptors. Endocytosis of the receptors is ubiquitin-independent - the endocytic adaptor protein extended-synaptotagmin can bind directly to FRS2 and mediates clathrin-mediated endocytosis [19, 20]. Not only the receptors underlie such regulation mechanisms, also the other proteins involved in the signaling pathway can be targets for inibitory mechanisms. Active ERK1 and 2 proteins for example have been shown to phosphorylate threonine and serine residues in the adaptor protein FRS2, resulting in its inability to recruit Grb2. Also various phosphatases, such as MAPK phosphatase 3 (MKP3) are induced to terminate the signaling [19]. The Sprouty proteins (SPRy) are endogenous inhibitors of FGF signaling. They act either as competitor for Grb2 binding, therefore preventing the binding of SOS and hence the activation of Ras, or by blocking the MAPK signaling via binding of Raf [19, 22].

1.2.3 Fibroblast Growth Factors and Cancer

Due to their multitude of functions during development, in wound healing and angiogenesis, it is not surprising that the deregulation of FGFs and/or their re-

ceptors can lead to severe alterations in an otherwise tightly regulated system. The overexpression of protein mediators which promote growth and survival is in general an important characteristic of cancer and one of the driving forces of tumor progression. FGFs in particular can support tumor growth and progression not only by inducing survival and growth of cells, but also through their function in angiogenesis, via induction of tumor vascularization [32].

It was shown in various cell models of different tumor types that FGFs and their receptors play an important role in tumor progression, malignant behavior, aggressive phenotypes and poor prognosis. FGF2, 5 and 18 for example were shown to be overexpressed in melanoma cell lines. Blocking of FGF signaling resulted in reduced cell proliferation and increased apoptosis [32]. In liver cancer FGF19 is among 18 tumor promoting genes which were found to be amplified in hepatocellular carcinoma cell lines [33]. In colorectal cancer it was found that the IIIc isoform of FGFR3 excerts oncogenic functions through binding and mediating the signaling of FGF18. In general it was found that FGFR3 is frequently deregulated in malignant epithelial cells, either through activating mutations, alterations in the splice variant or differential expression, leading to carcinomas. In carcinomas a switch from the IIIb isoforms, which is usually expressed on epithelial cells, to the IIIc isoform, which is found on mesenchymal cells, can frequently be observed. This enables the epithelial carcinoma cells to receive signals usually directed to mesenchymal cells, resulting in aggressive phenotypes [34]. In myelomas, bladder cancer and cervix cancer, activating mutations in the kinase domains or in the ligand-binding domains of FGFR3 were found [35]. In non-small cell lung cancer cell lines autocrine growth signal loops exist, which depend on FGF2 expression and signaling [36]. Autocrine FGFR signaling was also found in breast cancer cell lines, where the auto-stimulation results in a constitutively phosphorylated FRS2 and consequently in the constant activation of downstream signaling pathways promoting proliferation and survival [37].

1.3 Epithelial Mesenchymal Transition

Epithelial mesenchymal transition (EMT) is a process by which epithelial cells lose their specific epithelial attributes like apical-basal cell polarity and cell-cell-adhesion and gain mesenchymal features, like increased migratory and invasive abilities. This process plays an important role in embryonic development, adult tissue remodelling and in the development of cancer [10, 38].

In embryonic development EMT plays an important role during gastrulation. In this developmental stage EMT allows the cells to migrate into defined regions of the embryo to form the three primary germ layers ectoderm, endoderm and mesoderm. Cells can either migrate individually (complete EMT) or together with other cells (collective cell migration) through invagination or involution, for which a partial EMT is sufficient [38]. At their destination cells can undergo the reverse process, mesenchymal to epithelial transition (MET) to regain their epithelial characteristics and phenotype, and form a new epithelial layer [39].

One of the early events in EMT is the loss of cell-cell junctions, particularly the tight junctions and the cadherin-based adherens junctions. The cadherins, together with various anchor proteins are connected to actin filaments in the cells, thereby strengthening their connection [10, 38]. During EMT, the expression of E-cadherin is reduced by transcriptional repressors, namely Snail1 and Snail2 (Slug), which repress the transcription of E-cadherin via binding to E-boxes of the E-cadherin gene promotor, and ZEB1 and ZEB2 (zinc finger E-box-binding homeobox 1 and 2), which also bind to E-boxes [38] (for a more detailed description of those proteins and other EMT-markers see subsection 1.3.1 on page 12). Instead of E-cadherin, N-cadherin is expressed in mesenchymal cells, which leads to a weaker cell adhesion [40]. Also the actin filaments are re-organized during EMT, to form lamellipodia and filopodia for cell movement [38].

Another early event during EMT is the change of apicobasal cell polarity in epithelial cells to a front-rear polarity in mesenchymal cells. The interactions between cells and the ECM are important to define and maintain the tissue polarity, where the apical and basal surfaces implement different functions [39]. Since these interactions are weakened, and the epithelial basement membrane is disrupted, the epithelial cells undergoing EMT are prone to lose their typical polarity. The process in which the epithelial basement membtane is disrupted and the invasive mesenchymal cells penetrate into the ECM is called delamination [38, 39]. Mesenchymal cells in the ECM can synthesize and re-organize new components of the ECM and remodel it through the expression of various matrix metalloproteases (MMPs) [39].

A cell which has completely undergone EMT gains migratory and invasive properties as well as an elevated resistance against apoptosis. Such cells are capable of migrating away from the epithelial layer in which they originated [41]. Regarding the role of EMT in cancer, cells undergoing EMT acquire stem-cell like properties and play a role in immunosuppression and drug resistance [40].

The polarity of normal stem cells regulates the asymmetric division of those cells. A disturbance of the correct division (e.g through inappropriate induction of EMT) can lead to an abnormal cell division and an accumulation of dividing cells. This can result in cancer outgrowth by so called tumor initiating cells [10]. Cells in an epithelial layer undergoing EMT can compromise the integrity of the tissue and the organ function. Therefore, inappropriate induction of EMT greatly impairs the normal function of surrounding structures, contributing to cancer development. EMT is one key step in progression and metastasis of cancer due to various functions. Via remodelling of the EMC through mesenchymal cells, the primary tumor gains a protective tissue surrounding shielding it from the immune system. Additionally, cells undergoing EMT gain an increased resistance to apoptotic agents [39].

Mesenchymal cells produce various signaling proteins, including growth factors, to stimulate and sustain their mesenchymal phenotype. EMT-inducing proteins, such as growth factors like FGF, EGF, HGF or TGF-β, are produced and released by the cells, to stimulate various pathways inducing transcription factors needed to induce and maintain the mesenchymal state [39].

Various growth factors, e.g TGF-β, PDGF, HGF and EGF are known to induce EMT in specific cell lines in vitro [42]. In the colon cancer cell lines HT29 and DLD1 it was shown that treatment with EGF (20ng/ml) and/or FGF2 (10ng/ml) for several days induces EMT under serum-deprived conditions (see figure 5). The treatment increased the expression levels of ZEB1, snail1 and vimentin and reduced the level of E-cadherin expression which is typical for EMT [43]. Additionally it was shown that FGF2 modulates the expression of components of the TGF-β pathway, therefore promoting self-renewal in human embryonic stem cells [44]. A model for the role of EMT in tumorigenesis suggests that the tumor microenvironment produces TGF-β1, which promotes the tumor progression by inducing EMT [42]. These findings indicate a connection or even an interaction between the various growth factors and their contribution to stem cell-like properties of tumor cells and tumor progression.

The hepatocyte growth factor (HGF) induces cell scattering in the hepatocellular carcinoma (HCC) cell line HepG2 (see figure 6) via upregulation of Snail, which is a transcriptional repressor known to be involved in EMT [45]. Also an increased expression level of N-cadherin and a downregulation of E-cadherin in HepG2 and Huh7, another HCC cell line, was shown, suggesting a HGF-induced EMT in HCC [46].
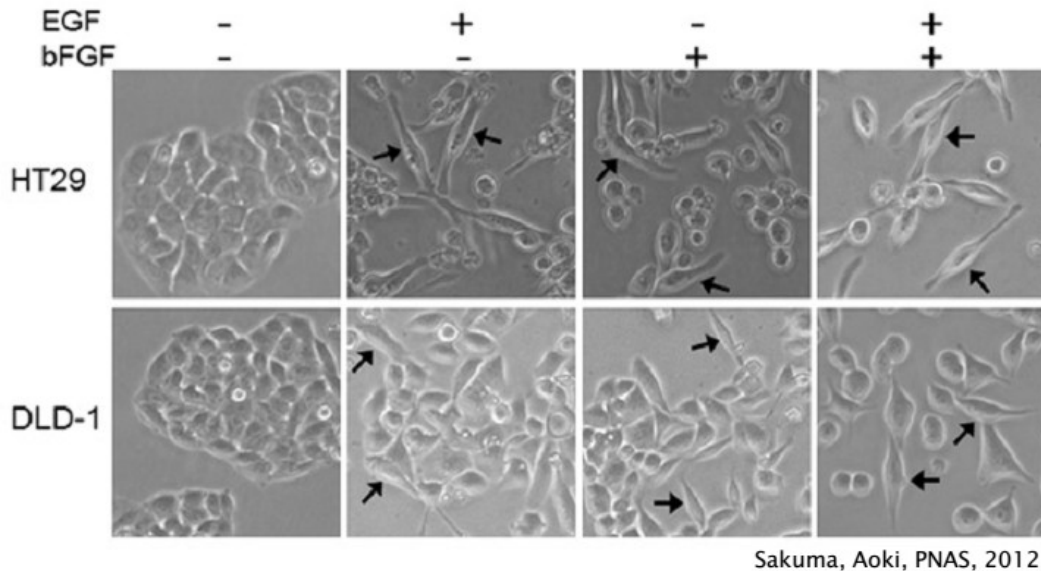

Figure 5: EMT in DLD-1 and HT29 cell lines, induced by treatment with either EGF or FGF2 or a co-treatment, image taken from Sakuma et al. [43].

11
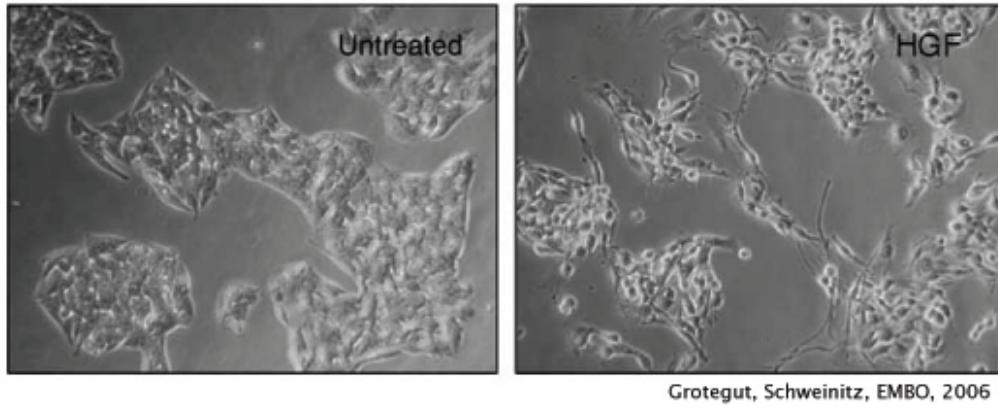
Figure 6: Scattering of HepG2 cells, induced by HGF treatment, image taken from Grotegut et al. [45].

1.3.1 EMT Markers

Important markers for EMT are the expression of E-cadherin and β-catenin in epithelial cells, and N-cadherin, vimentin, snail1, slug, ZEB1 and 2, as well as various matrix metalloproteinases (MMPs) in mesenchymal cells (see figure 7) [40].
E-cadherin is a calcium-dependent cell-cell adhesion glycoprotein. Its downregulation in mesenchymal cells decreases the strength of cellular adhesion, resulting in an increase in cellular motility. The downregulation of E-cadherin, e.g through transcriptional repression by the transcription factors ZEB1 or Snail1, occurs in various cancers at the onset of metastasis [43, 47]. The suppression of E-cadherin expression by ZEB1 is also an early event in EMT, therefore ZEB1 is also called an EMT-inducing transcription factor. β-catenin is on the one hand involved in the connection of the actin cytoskeleton to the cadherins in the cell membrane, which form the adherens junctions. Therefore it is mostly found in the epithelial cells where those junctions are more prominent. On the other hand it is involved in the Wnt-signaling pathway, which is involved in EMT activation and tumor progression [10].
Various transcription factors are known to induce EMT, among them are Snail1 and Slug, which are both zinc-finger proteins, ZEB1 and ZEB2, which are also zinc-finger proteins that bind to E-boxes to repress transcription, and Twist1, which is a basic helix-loop-helix protein [42].
During EMT the junctions between cells and ECM is weakened, and the cytoskeleton of the cells is reorganized. N-cadherin is also involved in the adherens junctions, but the expression of N-cadherin instead of E-cadherin leads to a weaker cell-cell adhesion [40, 47]. Vimentin, an intermediate filament, is the major cytoskeletal component of mesenchymal cells [47]. MMPs are zinc-containing, calcium-dependent endopeptidases which degrade extracellular matrix proteins like collagen or laminin. These extracellular proteases act only in the periphery

of the cells that produced them, and are needed for cell migration or to make room for dividing cells [47, 48]. MMPs are usually excreted by cells of the connective tissue and by pro-inflammatory cells, the expression is regulated by hormones, growth factors or cytokines [48]. Since MMPs degrade the ECM to let migrating cells through, they also play a role in tissue remodeling associated with tumor promoting processes such as metastasis and angiogenesis [49].

It was also found, that the miR-200 family of micro RNAs is downregulated during EMT, resulting in an upregulation of various genes involved in EMT, such as ZEB1 [42]. Especially miR-205 was shown to enforce an epithelial phenotype and its (over-)expression leads to a reduction of ZEB1 expression as well as an increase in the expression of E-cadherin [40].
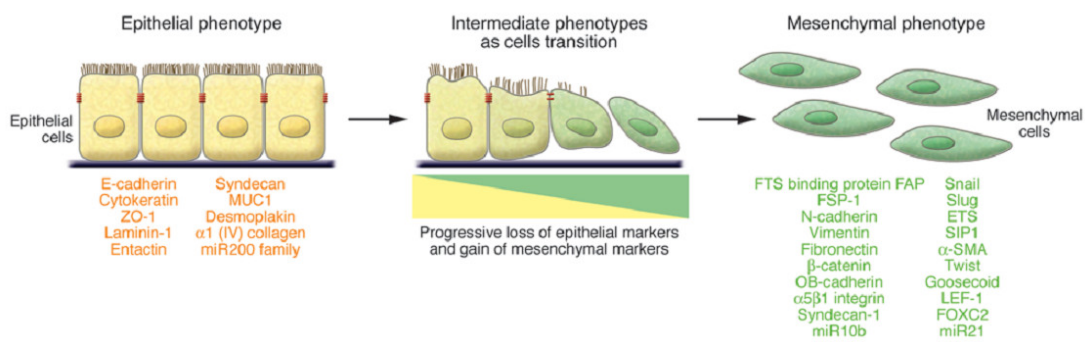

Figure 7: Epithelial to mesenchymal transition and typical EMT-markers, image taken from Kalluri and Weinberg [41].

1.3.2 EMT in Mesothelioma

As described earlier, malignant mesothelioma has 3 histological subtypes: the epithelioid, the biphasic or mixed, and the sarcomatoid subtype, the latter the most aggressive subtype with the worst prognosis. Between these subtypes a switch from epithelial markers in the epithelioid, to mesenchymal markers in the biphasic and sarcomatiod subtype was shown, suggesting EMT in those cells. Immunostaining and qRT-PCR showed a strong expression of E-cadherin in epithelioid MM, but only a weak expression in biphasic, and no expression in sarcomatoid MM. In addition, a strong expression of ZEB1 and vimentin in sarcomatoid cell lines was found [40]. In the biphasic subtype a downregulation of genes needed to control and maintain cell polarity was found. Also various genes needed for cell motility, e.g adaptor proteins needed for focal adhesions, were overexpressed. Genes such as Snail1, Slug, ZEB1 and Twist were also shown to be upregulated. These findings indicate a switch from the epithelial to a more aggresive mesenchymal phenotype in sarcomatoid and biphasic cells compared to the epithelioid cell lines [10].
Additionally, a significant downregulation of miR205, a microRNA which enforces

13

an epithelial phenotype via reduction of ZEB1 expression and upregulation of E-cadherin, was found in the biphasic and sarcomatoid subtypes [40].

1.4 Aims of study

FGF2 was already shown to induce various changes in some biphasic MPM cell lines, including morphology changes [12], and FGFs in general are known to contribute to EMT in other systems, for example FGF2 in colon carcinoma cell lines [43] or FGF10 in breast cancer cell lines [50]. The observed FGF2-induced changes in MPM cell lines could reflect a transition from epithelioid to sarcomatoid morphology and behavior with underlying EMT.

So the aims of this study are:

1. To characterize the FGF2-induced morphology changes in the two biphasic cell lines where they were previously observed, in detail checking the involved signaling pathways, the changes in gene expression as well as the changes in the behavior of the cells.

2. To evaluate how long FGF2 has to be present in the medium to induce the observed effects, whether these effects are dependent on the serum concentration in the medium and how long these effects are persistent after removal of the stimulus.

3. To answer the question whether the morphology changes in the two biphasic cell lines reflect a switch from the epithelioid phenotype and behavior to the more aggressive sarcomatiod behavior and more fibroblast-like phenotype, and whether the genes involved are also changed in epithelioid cell lines upon treatment, even though they do not show any morphology changes.

4. To determine whether the sarcomatiod cell lines are dependent on the pathway necessary for the induction of morphology changes also for their viability, or whether their sarcomatoid phenotype and behavior can even be reduced by inhibiting those pathways.

5. To investigate the growth factor induced EMT-like changes in additional MPM cell lines, as well as to further characterize various FGF2-regulated genes in MPM regarding their role in the aggressiveness of the tumor as well as in EMT.

2 Materials and Methods

2.1 Cell culture

The cells were cultured in T25 and T75 tissue culture flasks and maintained in RPMI, DMEM, MNP or MEME medium containing 10% FCS. The flasks were stored in a humidified atmosphere of 5% CO_2 at 37°C. The cells were passaged about twice a week in a ratio of 1:10 to 1:20 depending on the cell line.
Plates with seeded cells for the various assays were also kept in these conditions, unless otherwise stated.

2.1.1 Used cell lines

For a list of the used MPM cell lines see table 2, for other cell lines see table 3.

Table 2: Used MPM cell lines

Cell lines	Histological subtype	Standard growth medium	Source
SPC212	Biphasic MPM	RPMI + 10% FCS	R. Stahel University of Zurich
SPC111	Biphasic MPM	RPMI + 10% FCS	R. Stahel University of Zurich
M38K	Biphasic MPM	RPMI + 10% FCS	V. L. Kinnula University of Helsinki
p31	Epithelioid MPM	MEME + 10% FCS	K. Grankvist Umea University
P31res1.2	Epithelioid MPM	MEME + 10% FCS	K. Grankvist Umea University
VMC20	Epithelioid MPM	RPMI + 10% FCS	W. Klepetko Medical University Vienna
Meso62	Sarcomatoid MPM	DMEM + 10% FCS	W. Klepetko Medical University Vienna
Meso80	Sarcomatoid MPM	DMEM + 10% FCS	W. Klepetko Medical University Vienna
Meso84	Sarcomatoid MPM	RPMI + 10% FCS	W. Klepetko Medical University Vienna

Table 3: Non-MPM cell lines

Cell lines	Tumor type	Standard growth medium	Source
HT29	Human colon cancer cell line	MEME + 10% FCS	ATCC
DLD-1	Human colon cancer cell line	MEME + 10% FCS	ECACC
Hek293	Human embryonic kidney 293 cells	MEME + 10% FCS	ATCC
HepG2	Human hepatocellular carcinoma cell line	MNP + 10% FCS	ATCC

2.2 Molecular cloning and establishment of transgenic cell lines

2.2.1 Preparation of the vector

For creating plasmids carrying the FGF2 or the FGF18 transgene, the vector pQCXIP (Clontech) was used (see figure 8). First, about 3 μg vector were digested using the following restriction enzymes: 1 μl EcoR1 (1 FDU, FastDigest unit) and 1 μl Not1 (1 FDU) for the FGF2 insert, 2 μl Pac1 (2 FDU) for the FGF18 insert (Fermentas/Thermo Scientific). Vector and enzymes were mixed with 5 μl fast digest buffer (Fermentas/Thermo Scientific) and 33 μl dH$_2$O to a total of 50 μl and incubated at 37°C for 45 min. The digested vector was then precipitated with ethanol. For this, 150 μl 100% ethanol and 5 μl sodium acetate (3M, pH = 5) were added and the mixture was stored at -20°C for 2 h to over night. After this, the mixture was centrifuged at top speed and 4°C for 20 min. The supernatant was discarded and the pellet was washed with 500 μl 70% ethanol. This was again centrifuged at the same conditions for 5 min, the supernatant was discarded, the pellet air dried and then resuspended in 10 μl Tris-EDTA-buffer (TE-buffer, see table 4).

The concentration of the vector was determined by measuring the optical density at 260 nm, using a NanoDrop 1000 spectrophotometer (Peglab). After this, about 1 μg vector was mixed with 1 μl FastAP Thermosensitive Alkaline Phosphatase (1U), 2 μl 10x FastAP buffer (both from Fermentas/Thermo Scientific) and dH$_2$O to a total of 20 μl. The mix was incubated for 10 min at 37°C for dephosphorylation of the digested ends, to prevent religation of the vector in the ligation step. After the incubation the mixture was heated to 75°C for 5 min to inactivate the enzyme. 20 μl of the dephosphorylated vector were mixed with 6 μl vistra green and loaded on a preparative agarose gel (1%, for the composition of the gel and used reagents see section 2.4.1.1 on page 25). The gel was run for 10 min at 50 V, then for about 1 h at 110 V. After the run the bands were visualized by a Typhoon Trio FluorImager (GE Healthcare) and cut out of the gel with a scalpel. DNA was eluated from the gel slice using the Promega Wizard SV Gel and PCR clean-up system according to the manual. The concentration of the DNA was again measured using a NanoDrop 1000 spectrophotometer and the vector was then stored at -20°C.
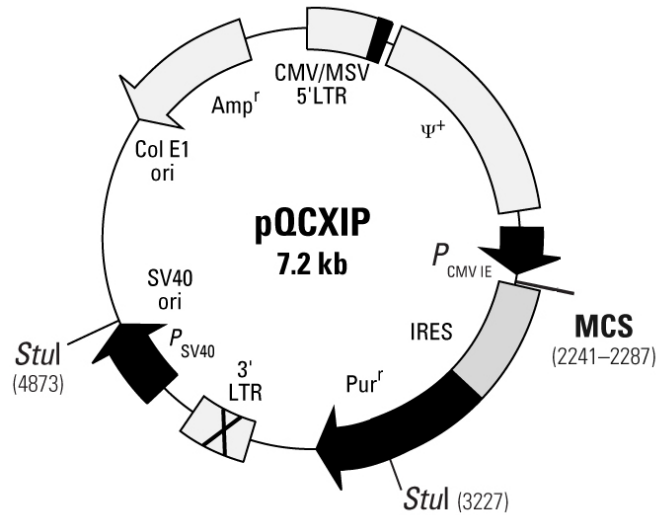
Figure 8: The vector pQCXIP (Clontech).

Table 4: TE-buffer

TE-buffer (pH = 7.4)
100 mM Tris-Cl pH = 7.4
10 mM EDTA pH = 8

2.2.2 Preparation of the insert

To generate the insert sequence for FGF2, a PCR with the cDNA of the untreated MPM cell line SPC212 was performed. For the components of the PCR mixture with the Pfu-polymerase see table 5. First, for an initial denaturation the samples were heated to 94°C for 3 min. Then, 40 cycles of denaturation (94°C, 50 sec), annealing (62°C, 50 sec) and elongation (72°C, 70 sec) were run in a BioRad Mycycler thermal cycler. After that, the samples were heated to 72°C for 3 min. For the primers used see table 6.
The size of the PCR product was checked on an agarose gel. After confirmation of the right size of the product, about 40-50 µl of the samples were run on a 1% preparative agarose gel, the bands were cut from the gel and eluted using the Promega kit, as described for the vector. Then the DNA fragments were digested with the appropriate restriction enzymes to fit the vector ends; 40 µl of the eluted DNA were mixed with 3 µl dH$_2$O, 5 µl fast digest buffer and 1 µl of each restriction enzyme (Not1 and EcoR1). The mix was incubated for 45 min at 37°C. After the incubation time, the DNA was again separated on a 1% preparative agarose gel, the DNA bands were cut and the DNA was eluted using the Promega kit. The concentration of the DNA was determined using a NanoDrop 1000 spectrophotometer and the samples were then stored at -20°C.

17

Table 5: Components of the PCR mixture with the Pfu-polymerase

Preparation of the PCR mix (total 50 µl)

40.5 µl dH$_2$O
5 µl 10x Pfu reaction buffer + MgSO$_4$ (Thermo Scientific)
1 µl dNTPs, 10 mM each (final conc. = 200 µM)
1 µl hsFGF2 18kDa forward primer (final conc. = 0.4 µM)
1 µl hsFGF2 18kDa reverse primer (final conc. = 0.4 µM)
1 µl SPC212 cDNA
0.5 µl Pfu-Polymerase (2.5U/ µl)

Table 6: PCR primers

Name	Sequence	Annealing temp
hsFGF2 18kDa for2	TTAGCGGCCGCATGGCAGCCGGGAGCA	60.8°C
hsFGF2 18kDa rev1	TTTGAATTCAGCTCTTAGCAGACATTG	60.8°C
hsFGF18 Pac for	TTTTTAATTAACGATGTATTCAGCGCCCTC	62°C
hsFGF18 Pac rev	TTTTTAATTAACCTAGGCAGGGTGTGTG	62°C

For the FGF18 insert a Q5-polymerase instead of the Pfu-polymerase was used. Also, instead of cDNA from the SPC212 cell line, a vector with FGF18 already inserted was used (for a complete list of the components used see table 7, for the primers used see table 6). The PCR machine was preaheated to 98°C for the initial denaturation (50 sec), then 35 cycles of denaturation (98°C, 10 sec), annealing (62°C, 20 sec) and elongation (72°C, 20 sec) were run. Afterwards the samples were heated to 72°C for 2 min. The size of the PCR products was checked on a 1% agarose gel and the DNA was precipitated with 100% ethanol as described for the vector. The DNA was then digested as described for the FGF2 insert, using 2 µl of the Pac1 restriction enzyme instead of EcoR1 and Not1. Also separation on an agarose gel and eluation was performed as described before. The insert was then stored at -20°C.

Table 7: Components of the PCR mixture with the Q5-polymerase

Preparation of the PCR mix (total 50 µl)

10 µl 5x Q5 buffer (New England Biolabs, NEB)
1 µl dNTPs, 10 mM each (final conc. = 200 µM)
1.25 µl hsFGF18 Pac forward primer (final conc. = 0.5 µM)
1.25 µl hsFGF18 Pac reverse primer (final conc. = 0.5 µM)
0.5 µl Q5-polymerase (0.02 U/ µl; NEB)
0.5-1 µl DNA (<1 ng)
35.5-35 µl dH$_2$O

2.2.3 Ligation and transformation

For ligation of the inserts with the vectors 100 ng of vector were mixed with the insert in a 1:3 or 1:6 ratio, and 2 µl T4 DNA ligase buffer, 2 µl T4 DNA ligase (Thermo Scientific) and dH$_2$O to a total of 20 µl were added. As a negative control, only 100 ng of the vector were mixed with ligase, buffer and dH$_2$O to a total of 10 µl. The samples were kept at 16°C over night.

For transformation of competent E.coli, 100 µl competent bacteria were added to 3 µl of the constructs and kept on ice for 20 min. Then the bacteria were heat shocked at 42°C for 60 sec and briefly put on ice again. 1 ml SOC medium (see table 8) was added, and the bacteria were incubated on a shaker (300 rpm) for 1-2 h at 37°C. After that, the samples were centrifuged at 4000 rpm for 3 min, the supernatant was discarded and the pellet resuspended in about 150 µl SOC medium. This was plated on an agar plate containing ampicillin for selection of construct-carrying bacteria (see table 9). The agar plates were then incubated at 37°C over night.

Table 8: SOC medium (=SOB Medium containing 20 mM glucose)

SOC medium, pH = 7
20 g Tryptone (Sigma-Aldrich)
5 g Yeast extract
0.5 g NaCl
10 ml KCl 250 mM
5 ml MgCl$_2$ (2 M)
dH$_2$O to a total of 1 L
20 ml Glucose solution (1 M)

Table 9: Agar plates with ampicillin for E.coli

Agar plates
20 g LB-broth (Sigma-Aldrich)
15 g Agar (Sigma-Aldrich)
dH$_2$O to a total of 500 ml
500 µl Ampicillin (final conc. = 0.1 mg/ml)

On the next day colonies (up to 20 per plate) were picked and each one put into 2 ml LB-medium (see table 10) containing ampicillin (final conc. = 0.1 mg/ml). The tubes were then again incubated at 37°C over night and on the next day the plasmids were isolated.

Table 10: LB-medium (Luria-Bertani medium), pH = 7

LB-medium
10g Tryptone (Sigma-Aldrich)
5g Yeast extract
10g NaCl
dH$_2$O to a total of 1 L

2.2.4 Plasmid isolation "quick 'n' dirty"

1.5 ml of the overnight culture were transferred into a 1.5 ml tube and centrifuged at 1.6 x 10^4 g for 1 min. The supernatant was discarded and the pellet resuspended in 700 µl STET-buffer (see table 11). 13 µl lysozyme (10 mg/ml) were added and mixed by inverting the tube. The samples were then heated to 100°C for 2 min and again centrifuged at 1.6 x 10^4 g for 10 min. 500 µl of the supernatant containing the plasmid were then transferred into fresh tubes containing 1 µl RNaseA (concentration = 10 mg/ml) and mixed by inverting the tubes. 700 µl isopropanol were added to each tube and the samples were transferred to -20°C for 20 min to precipitate the DNA. After centrifugation at 4°C and 1.4 x 10^4 rpm for 15 min, the supernatant was discarded and the pellet washed in 500 µl 70% ice cold ethanol. After another centrifugation step (top speed for 5 min at room temperature), the supernatant was discarded and the dry pellet was resuspended in 15 µl TE-buffer. The samples were stored at -20°C.

Table 11: STET-buffer

STET-buffer
25 ml 1 M Tris/HCl pH = 8 (final conc. = 50 mM)
50 ml 0.5 M EDTA pH = 8 (final conc. = 50 mM)
40 g Sucrose
dH$_2$O to a total of 475 ml
25 ml TritonX (added after autoclaving)

2.2.5 Midiprep plasmid isolation

The isolated plasmids were digested with restriction enzymes which cut in the vector and in the insert (yielding fragments of defined sizes), to determine if the insertion was successful and in the right orientation. For this, the fast digest enzymes BamH1 and BglII were used. The digested DNA was then loaded on a 1% agarose gel to determine the size of the fragments.
100 µl of the overnight cultures containing plasmids which gave the correct fragments were mixed with 100 ml LB-medium containing ampicillin (final conc. = 0.1 mg/ml) and put on a shaker at 37°C over night. On the next day, a midiprep

plasmid isolation with the Promega PureYield plasmid midiprep system was performed as recommended in the manual. The plasmids were again digested and loaded on a gel for control, then sent to sequencing by a commercial service (Eurofins).

2.2.6 Creation of the virus

For producing the retroviral particles, 2×10^6 Hek293 cells were seeded into one T25 flask and left to recover over night. On the next day the medium was changed and the transfection reagents were prepared. 625 µl Optimem 1 medium were mixed with 25 µl Lipofectamine 2000 (both from Invitrogen) and incubated for 5 min at room temperature. Meanwhile 625 µl Optimem 1 medium were mixed with 3.75 µg of a plasmid carrying the pGagPol sequence and 1.25 µg of a plasmid carrying the pVSVG sequence, both needed for virus assembly. Also 5 µg of the plasmids carrying FGF2 or FGF18 respectively, were added. Both mixtures were then combined and incubated for another 20 min at room temperature. After the incubation, the reagents were added to the T25 flask containing the Hek293 cells.

After 5 h the medium was changed to a fresh medium containing 10% serum, and the cells were cultured for another 48 h. After 48 h the medium containing the virus was filtrated and aliquoted (1 ml each) in 1.5 ml tubes. The aliquots were stored at -20°C.

2.2.7 Retroviral transduction

For transducing the cells, 3×10^4 cells were seeded in a 6-well plate and left to recover over night. On the next day, the growth medium in the wells was removed and one aliquot of the required virus (1 ml medium containing the virus) was added. Also 4 µl polybrene were added to each well (final concentration: 8 µg/ml). The virus was kept on the cells for 5-24 h. After the incubation time, the medium in the wells was again changed to a growth medium containing 10% serum, and antibiotics were added for selection (puromycin for the FGF2 and FGF18 vectors, neomycin for the RFP vectors). Puromycin was added at a final concentration of 0.8 µg/ml, neomycin was added at a final concentration of 500 µg/ml. As a control for selection efficiency, the antibiotics were also added to non-transfected cells.

After 1-2 weeks the colonies formed under the selection pressure were transferred into a fresh T25 flask and kept in the incubator at 37°C. Antibiotics for sustaining the pressure to keep the transgene were added after every 3rd to 4th passage.

2.3 Growth factors and inhibitors

10^5 cells were seeded per well of a 6-well plate and left to recover over night in 2 ml medium containing 10% serum. On the next day, the cells were treated

with various inhibitors (see table 12) and/or growth factors (see table 13) with different concentrations. For some experiments the growth medium was changed after 24 h to a starvation medium containing only 0.1-0.5% serum or no serum at all. Treatment was then added after another 24 h.

Depending on the purpose, inhibitors were removed after one to 24 h, whereas growth factors were removed after one minute, five minutes, 15 min, one hour or not at all. Pictures were taken after 24 to 72 h using a Nikon Eclipse Ti-S microscope.

Table 12: Inhibitors

Inhibitor	Target	Conc.
Ponatinib	Tyrosine kinases (multiple)	0.5 µM
Erlotinib	Tyrosine kinase domain of the EGF-Receptor	10 µM
Selumetinib	MEK	10 µM
PD166866	Tyrosine kinase domain of the FGF-Receptor 1	10 µM
MK2206	AKT	10 µM
LY294002	PI3-kinase	20 µM
UO126	MEK	10 µM
SB431542	TGFβ and activin receptors	20 µM

Table 13: Growth factors

Growth factor	Full name	Receptor(s)	Concentration
FGF1 (acidic FGF)	Fibroblast growth factor 1	FGFR1-IIIb and IIIc FGFR2-IIIb and IIIc FGFR3-IIIb and IIIc FGFR4	10 ng/ml
FGF2 (basic FGF)	Fibroblast growth factor 2	FGFR1-IIIb and IIIc FGFR2-IIIc FGFR3-IIIc FGFR4	10 ng/ml
FGF5	Fibroblast growth factor 5	FGFR1-IIIc FGFR2-IIIc FGFR3- IIIc FGFR4	10 ng/ml
FGF18	Fibroblast growth factor 18	FGFR1-IIIc FGFR2-IIIc FGFR3- IIIc FGFR4	10 ng/ml
HGF	Hepatocyte growth factor	c-Met	10 ng/ml
EGF	Epidermal growth factor	EGFR	10 ng/ml
PDGF-ab	Platelet-derived growth factor	α- and β-type PDGFR	10 ng/ml
BMP2	Bone morphogenetic protein 2	BMPR1A	10 ng/ml
Activin A		ACVR1, ACVR1B, ACVR1C, ACVR2A, ACVR2B	10 ng/ml
TGF-β-1	Transforming growth factor β 1	TGF-β receptor 1 and 2	10 ng/ml

2.3.1 Quantification of the morphology changes

To quantify the morphology changes of the biphasic MPM cell line M38K upon treatment with growth factors and/or inhibitors, two approaches were applied.

2.3.1.1 By measuring and counting contiguous cell clusters

For the purpose of counting and measuring contiguous cell clusters, the pictures of treated and untreated cells were edited with Adobe Photoshop CS4. Background area was colored in black, whereas cell areas were colored in white. The area of the white, respectively black areas was measured using the Magic Wand tool and the Analyze tool of Photoshop. After the measurement, contiguous cell clusters were counted using the Counting tool.
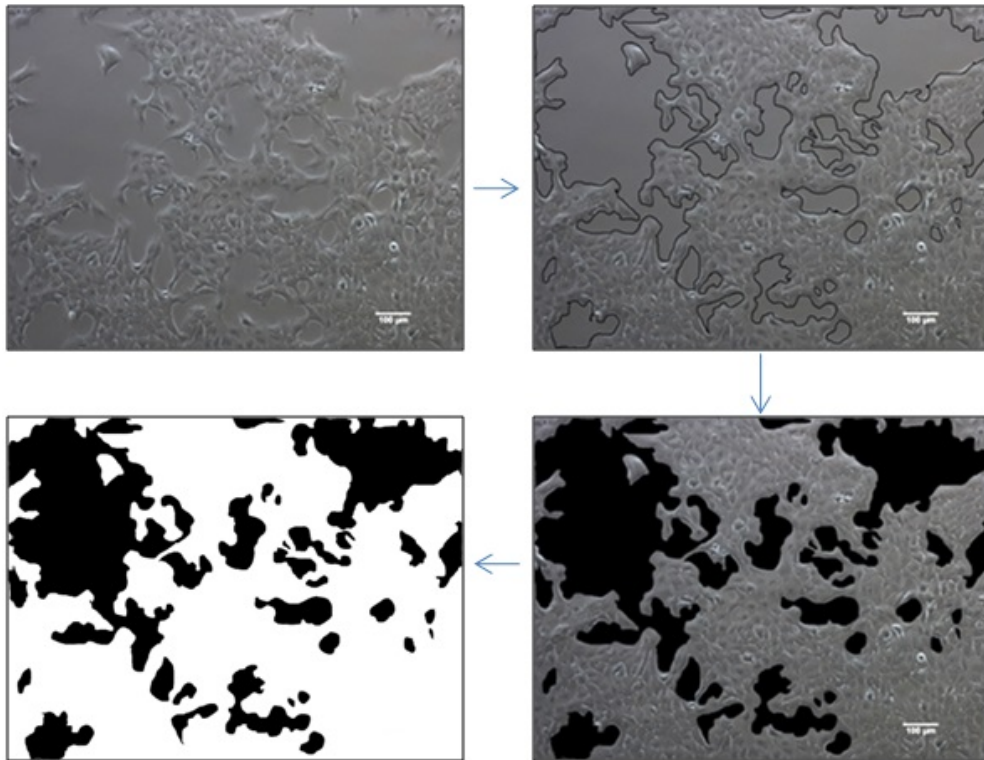

Figure 9: Coloring the background and the cell area with Adobe Photoshop CS4.

2.3.1.2 By measuring the percentage of cell-cell and cell-background contacts

For this quantification method, the pictures of treated and untreated cells were randomly divided into small areas, three squares were chosen and ten cells out of these squares were measured. With the Freehand Lines tool, the length of cell-cell borders was measured, as well as the length of cell-background borders. The measured lengths were then transferred into an excel-file and the perimeter of one cell as well as the percentage of cell-cell and cell-background contacts were calculated.

To ensure randomness of the region to measure, 3 coordinates of the grid were chosen before looking at the picture. Then, the grid was randomly inserted using the grid plugin of ImageJ with the option "random offset" and 10 cells were

measured in the chosen grid.
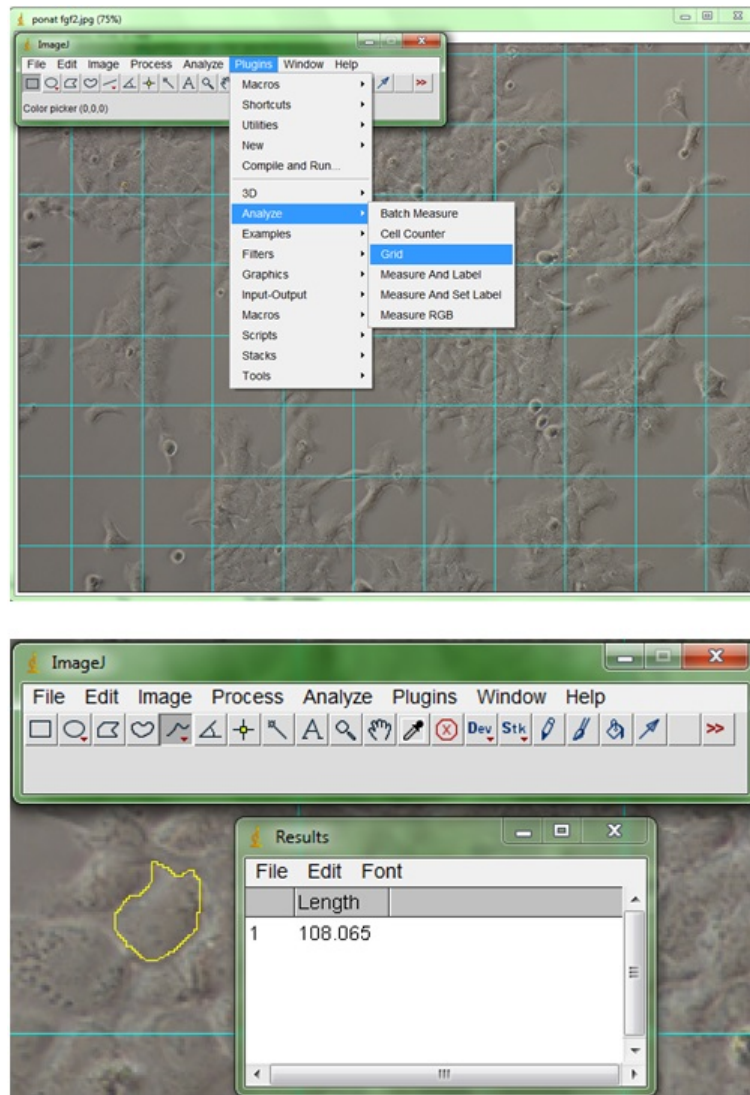
Figure 10: Randomly dividing the picture into smaller regions and measuring the length of cell-cell contact using the Freehand Lines tool.

2.4 Expression analysis

2.4.1 RNA isolation

For RNA isolation, 10^5 cells were seeded in a 6-well plate and left to recover over night. Cells were then either treated and incubated for another 24 h, or, in case of the transgenic cell lines, only incubated for another 24 h without treatment. Then the medium was removed and 2 ml trizol (see table 14) were added to each well. The cells were scraped off and transferred into 1.5 ml tubes, 1 ml each. 200 µl chloroform per 1 ml trizol were added and mixed by vortexing the

tubes. The suspension was then centrifuged at 4°C and 1.3 x 10^4 g for 20 min, resulting in three phases, where the upper aqueous phase contains the RNA. This phase was transferred into a new 1.5 ml tube (approx. 500 µl), 500 µl isopropanol were added and mixed by vortexing. For precipitation of the RNA the tubes were transferred to -20°C over night. Then the samples were again centrifuged for 10 min, at 4°C and 1.3 x 10^4 g, the supernatant was discarded and the pellet was washed with 1 ml 75% ethanol. After another centrifugation step for 5 min at 4°C and 1.3 x 10^4 g, the ethanol was removed and the tubes were left open to air-dry the pellet (approx. 15 min). Finally the RNA was dissolved in 15 µl nuclease-free dH_2O, heated to 60°C for 5 min and then stored at -80°C.

The RNA concentration was determined by measuring the optical density at 260 nm, using a NanoDrop 1000 spectrophotometer (Peqlab). Furthermore the quality of the RNA was checked on a 1.5% agarose gel.

Table 14: Trizol

Trizol
0.8 M Guanidine thiocyanate
0.4 M Ammonium thiocyanate
0.1 M Sodium Acetate
5% v/v Glycerol
38% Phenol

2.4.1.1 Agarose gel electrophoresis

For separation of nucleic acids (DNA, RNA) according to their length (bp), gel electrophoresis was used. For size determination, 1 kb or 100 bp DNA ladders (Fermentas) were used.
For RNA samples, a 1.5% agarose gel was prepared. 1 µg of RNA in 5 µl nuclease-free ddH_2O were mixed 1:1 with urea buffer (see table 15) and denatured at 70°C for 3 min. For staining of the RNA bands, 2 µl of vistra green (see table 16) were added to each sample, and the RNA was loaded onto the gel, placed in the electrophoresis tank filled with TBE (see table 17). The gel was run at 50 V for 10 min and then at 100 V for 20-35 min. The bands were visualized by a Typhoon Trio FluorImager (GE Healthcare), which detects the flourescence of the vistra green bound to nucleic acids.

Table 15: Urea buffer

Urea buffer
2 x TBE
7 M Urea
15% Glycerol

Table 16: Vistra green loading dye (6x)

Vistra green
666 µl 6x Loading dye (Fermentas)
700 µl dH$_2$O
500 µl 80% Glycerol
133 µl 0.5 M EDTA
1 µl Vistra-green 10000x (Amersham)

Table 17: TBE - Tris borate EDTA buffer

TBE
10.8 g/l Trizma base (Sigma)
5.5 g/l Boric acid (Sigma)
4 ml/l 0.5M EDTA, pH = 8.0
dH$_2$O to 1 L

2.4.2 Synthesis of cDNA

For cDNA synthesis, 2 µg RNA were mixed with ddH$_2$O to a total of 13 µl. The samples were heated to 70°C for 10 min to denature and then put on ice for 10 to 15 min to cool down. Then 7.5 µl of cDNA master mix (see table 18) were added to a total of 20.5 µl and the samples were incubated at 42°C for 1 h. To stop the reaction, the enzyme was denatured at 70°C for 10 min. Finally 20 µl RNase free ddH$_2$O were added to dilute the samples 1:1. The samples were stored at -20°C for up to two weeks, or at -80°C.

Table 18: 1 x cDNA master mix

1 x cDNA master mix
4 µl 5 x M-MLV RT buffer (Fermentas)
1 µl dNTPs (10 mM, Fermentas)
1 µl Reverse transcriptase (200 U/µl, Fermentas)
0.5 µl Riboloc RNase inhibitor (40 U/µl, Fermentas)
1 µl Random hexamer primers (0.5 µg/µl, Fermentas)

2.4.3 Quantitative real-time Polymerase Chain Reaction (qPCR)

To confirm the expression levels of FGF2 and FGF18 in the transgenic cell lines, as well as expression changes of other genes upon FGF2 or EGF treat-

ment according to the microarray data, quantitative real-time Polymerase Chain Reaction (qPCR) was used.

2.4.3.1 TaqMan qPCR

For a semi-quantitative analysis of the transcript levels of the transgenes in the transfected M38K and SPC212 cell lines, TaqMan qPCR was performed. For this, 1 µl cDNA was mixed with 11.5 µl of TaqMan qPCR Master Mix (see table 19), containing the appropriate TaqMan probe in a MicroAmp Optical 96-well Reaction Plate (Applied Biosystems). The plate was then placed in an ABI Prism 7000 SDS Thermocycler (Applied Biosystems) and the PCR program was started (see table 20). Fluorescence was measured after every cycle. As references for normalization, two housekeeping genes GAPDH and β-2-Microglobulin (b2M) were used. The PCR products were then verified by agarose gel electrophoresis. The preparations for the qPCR were done in duplicates and on ice. For a list of all TaqMan probes used see table 21.

Table 19: 1 x TaqMan qPCR Master Mix

1 x TaqMan qPCR Master Mix
6.25 µl Maxima Probe qPCR Master-Mix (Fermentas)
0.625 µl TaqMan probe(Applied Biosystems)
4.625 µl dH$_2$O

Table 20: Standard conditions for TaqMan qPCR

	Temperature	Time (minutes)	Repetitions
Stage 1	50°C	02:00	1x
Stage 2	95°C	10:00	1x
Stage 3	95°C	00:15	40x
	60°C	01:00	

Table 21: TaqMan probes used for expression analysis

Target	Assay ID
FGF2	Hs00960934 m1
FGF18	Hs00826077 m1
GAPDH	Hs99999905 m1
b2M	Hs00984230 m1

2.4.3.2 SYBR Green qPCR

To confirm the changes in gene expression upon treatment with FGF2 or EGF observed in the microarray data of treated M38K and SPC212 cell lines, primers for eight different genes with high expression level changes were designed, using the program clone manager. For this, the mRNA sequence of the genes of interest was taken from the NCBI.nlm.nih.gov website, the primers were designed using the "primer design" function of clone manager. The GC% range was set to a minimum of 40 and a maximum of 70, the optimal length of the primers was set to 20. The acceptable product length was set between 90 and 150 bp. The best primer pair according to the ranking of the program was chosen. These eight primers as well as other, not self-designed primers were used for the SYBR Green qPCR. For a list of the used primers see table 22.

Table 22: Primer for the SYBR Green qPCR

Target	Sense	Primer Sequence	Annealing Temp.	Product Size (bp)
BDKRB2	forward	CGGCCTCTTTCAGCGCCGAC	56°C	106
	reverse	AGCCAGCCCAGCCACTCCAC		
CD274	forward	CACCACCAATTCCAAGAG	47°C	143
	reverse	CTGGGATGACCAATTCAG		
ESM1	forward	GTGGACTGCCCTCAACAC	53°C	147
	reverse	GCCATCCATGCCTGAGAC		
E-Cad*	forward	CAGAGCCTCTGGATAGAGAACGCA	58°C	245
	reverse	GGCATTGTAGGTGTTCACATCATCGTC		
ETV4	forward	CCGGCCAGCCATGAATTAC	54°C	142
	reverse	CGGGAAGGCCAAAGAGAAGAG		
GAPDH	forward	CTGGCGTCTTCACCACCAT	55°C	499
	reverse	GCCTGCTTCACCACCTTCT		
GATA6	forward	GTGCCCAGACCACTTGCTAT	46°C	106
	reverse	TGGAATTATTGCTATTACCAGAGC		
ITGA6	forward	GCTCCCAGAGCCAATCAC	51°C	129
	reverse	CACCGCCACATCATAGCC		
LAMC2	forward	AGCCAAGAGAACAGCTACC	50°C	116
	reverse	GTGATGAGCCTGTGAGTATCC		
MMP1	forward	TACATGCGCACAAATCCC	49°C	149
	reverse	ACAGCCCAGTACTTATTCCC		
MMP3	forward	TGGGCCAGGGATTAATGGAG	50°C	110
	reverse	GGGAGTGGCCAATTTCATGAG		
SMAD7	forward	TGCCTTCCTCCGCTGAAAC	54°C	128
	reverse	CGTCTTCTCCTCCCAGTATGC		
SNAIL1*	forward	TATGCTGCCTTCCCAGGCTTG	57°C	143
	reverse	ATGTGCATCTTGAGGGCACCC		
Vimentin*	forward	GGCTCAGATTCAGGAACAGC	55°C	373
	reverse	CTGAATCTCATCCTGCAGGC		
ZEB1*	forward	CCAGTGGTCATGATGAAAATGGAACACC	58°C	243
	reverse	CAGACTGCGTCACATGTCTTTGATCTC		

Primers marked with an asterisk are taken from Sakuma et al. [43].

2.4.3.3 Creating a heatmap for visualizing qPCR data using R

To create a heatmap for better visualisation of the SYBR green qPCR results, R was used (R - Version 3.1.0, "Spring Dance"; released 10.04.2014; Platform: x86_64-pc-linux-gnu (64-bit)). The following script was applied:

```
> library("gplots")
> library("RColorBrewer")
> data <- read.csv("data_new.csv")
> rnames <- data[,1]
```

```
> x <- data.matrix(data[,2:ncol(data)])
> rownames(x) <- rnames
> mycolors <- colorRampPalette(c("green", "black", "red"))
  (n=299)
> col_breaks = c(seq(0,0.9,length=100), seq(0.9,1.1,length
  =100), seq(1.1,1000,length=100))
> png("heatmap_final.png", width=1000, height=1000, res
  =300, pointsize=7)
> heatmap.2(x, main = "PCR_Data", col = mycolors, breaks =
   col_breaks, margins = c(12,12), trace = c("none"))
> dev.off()
```

2.5 Protein analysis

2.5.1 Protein isolation

For total protein isolation, 3 x 10^5 cells were seeded in each well of a 6-well plate and grown over night in 2 ml medium. After the treatment (15 min to 24 h), cells were put on ice, the medium was removed and the cells were washed with cold PBS. 50-60 µl lysis buffer (LBII, see table 23) were added, the cells were scraped off and transferred into a 1.5 ml tube. The suspension was sonicated for 5 min and afterwards centrifuged for 5 min at 1.2 x 10^4 g and 4°C. The supernatant was transferred into a new 1.5 ml tube and stored at -20°C.

Table 23: Protein Lysis Buffer II

Stock solution	Final Concentration	1 Liter (+bdH₂O)	10 ml (+bdH₂O)
100 mM EGTA	1 mM EGTA	10 ml	100 µl
5M NaCl	150 mM NaCl	30 ml	300 µl
50 mM Na₃VO₄	1 mM Na₃VO₄	20 ml	200 µl
100% Triton X	1% Triton X	10 ml	100 µl
100 mM NaF	10 mM NaF	100 ml	1 ml
1M Tris pH=8	50 mM Tris pH=8	50 ml	500 µl

2.5.2 Protein supernatant precipitation

To analyze whether FGF2 or FGF18 was secreted by the transgenic cell lines, a western blot with precipitated proteins was performed. For this, the cells were grown in 5 ml medium containing 10% serum in a T25 flask until they were about 80% confluent. Then the medium was removed, the cells were washed twice with PBS and 5 ml of serum-free medium were added. Cells were then kept in the serum-free medium for 24 h. After that, the medium was transferred into a falcon

tube and centrifuged at 100 g for 5 min to pellet the cells in the medium. The supernatant was then transferred to a new tube, and 4 volumes of acetone were added. The tubes were then stored at -20°C over night. On the next day the mixture was centrifuged at 4°C and 1.5 x 10^4 g for 10 min, the supernatant was discarded and the pellet resuspended in 1 ml 100% EtOH. The mixture was again centrifuged at 4°C and 1.5 x 10^4 g for 10 min, the EtOH was removed and the tube was left open to air-dry the pellet for about 5-10 min. Then the pellet was resuspended in the appropriate amount of LBII (lysis buffer, see table 23) and stored at -20°C.

2.5.3 SDS Page

Gel electrophoresis was used to separate the proteins according to their molecular weight (kDa). 15-30 μg of protein were mixed with ddH$_2$O to a total of 20 μl. 5 μl 5 x reducing Laemmli buffer (see table 24) with β-mercaptoethanol were added. After denaturation at 100°C for 5 min, the samples were centrifuged and loaded on a polyacrylamide gel, either a discontinuous gel consisting of a 10% or 15% separating gel and a 5% stacking gel (composition of the gel see table 25), or a precast gel from NuSep. The gels were placed in an electrophoresis tank filled with SDS running buffer (see table 26) prior to loading with the samples. The gel was run at 60 V for 15-25 min and then at 110 V for about 1 h.

Table 24: 5 x reducing Laemmli buffer with β-mercaptoethanol

Laemmli buffer
300 mM Tris.Cl pH = 6.8
60% Glycerol
10% SDS
0,025% Bromphenolblue
7% β-mercaptoethanol

Table 25: Composition of the stacking gel and the separating gel

5% Stacking gel (2 gels)	10% (15%) Separating gel (2 gels)
3.6 ml ddH$_2$O	5.88 ml (3.368 ml) ddH$_2$O
0.625 ml Tris 0.5 M (pH = 6.8)	3.75 ml Tris 1.6 M (pH = 8.8)
0.1 ml 10%SDS	0.3 ml 10% SDS
0.625 ml 30% Acrylamid/Bis; 29:1(Bio-Rad)	5.025 ml (7.538 ml) 30% Acrylamid/Bis; 29:1(Bio-Rad)
50 μl APES	37.5 μl APES
75 μl TEMED (Amresco)	20 μl TEMED (Amresco)

Table 26: SDS running buffer

SDS running buffer
25 mM Tris base
192 mM Glycine
0.1% SDS

2.5.4 Western blot

To transfer the proteins from the gel to a PVDF-Membrane (Hypond-P, GE Healthcare), a Mini Protean 3 System was used, according to the instructions of the manufacturer. The transfer of the proteins was performed in Towbin Transferbuffer (see table 27), either over night at 4°C and 18 V, or for 1 h and 15 min at 4°C and 300 mA. To check the quality of the transfer, the membrane was stained for 15-60 min with Ponceau S and afterwards blocked in 5% nonfat dried milk in TBST (TBS containing 0.1% Tween, see table 28) for 1-4 h. Then the membrane was incubated in the primary antibody over night at 4°C (complete lists of the used primary and secondary antibodies are shown in table 29 and table 30). On the next day the membrane was washed 3 x 10 min with TBST and incubated in the secondary antibody for about 2 h at room temperature. After the incubation, it was again washed 3 x 10 min with TBST and 15 min with TBS once. The antibody binding was visualized on x-ray films using Immune-Star WesternC Kit (Bio-Rad) as recommended in the manual. Exposure times varied between one second and 50 min depending on the antibody and the strength of the signal.

Table 27: Towbin transfer buffer

Towbin transfer buffer
13.39 g/l Glycine
3.03 g/l Tris base
50 ml/l Methanol

Table 28: TBS - Tris-buffered saline

TBS
8 g/l NaCl
0.2 g/l KCl
3 g/l Tris base
HCl to adjust pH to 7.4
(approx. 15 ml)

Table 29: Primary antibodies used for the western blot

Antibody	Dilution and Diluent	Target size	Assay ID
Rabbit anti-Erk 1/2	1:1000 in 5% BSA in TBST	42/44kDa	Cell Signalling, #9102
Rabbit anti-pErk 1/2	1:1000 in 5% BSA in TBST	42/44kDa	Cell Signalling, #9101
Rabbit anti-AKT	1:1000 in 5% BSA in TBST	60kDa	Cell Signalling, #9272
Rabbit anti-pAKT	1:1000 in 5% BSA in TBST	60kDa	Cell Signalling, #9271
Rabbit anti-S6	1:1000 in 3% BSA in TBST	30 kDa	Cell Signalling, #2217
Rabbit anti-pS6	1:1000 in 3% BSA in TBST	30 kDa	Cell Signalling, #2215
Rabbit anti-PLCγ1	1:1000 in 5% BSA in TBST	155 kDa	Cell Signalling, #2822
Rabbit anti-pPLCγ1	1:1000 in 5% BSA in TBST	155 kDa	Cell Signalling, #2821
Rabbit anti-FGFR1	1:1000 in 5% milk in TBST	92, 120, 145 kDa	Cell Signalling, #9740
Rabbit anti-pFGFR1 (y653/654)	1:1000 in 3% BSA in TBST	120 kDa	Thermo Scientific PA512594
Rabbit anti-FGF2	1:1000 in 3% BSA in TBST	19 kDa	SantaCruz, sc-7911
Goat anti-FGF18	1:200 in 3% BSA in TBST	24kDA	SantaCruz, sc-16830
Mouse anti-β-Actin	1:10000 5% BSA in TBST	42kDa	Sigma, #A 5441

Table 30: Secondary antibodies used for the western blot

Antibody	Dilution and Diluent	Supplier
Polyclonal Goat anti-Rabbit Immunoglobulins/HRP	1:10000 in 5% milk in TBST	Dako
Anti-Mouse HRP	1:10000 in 5% milk in TBST	Dako

2.5.4.1 Membrane stripping

When needed, the membranes were stripped, meaning the primary antibodies already used and still bound on the membrane were removed. For this, the membranes were washed 2 x 10 min in Abcam stripping buffer (see table 31), afterwards 2 x 10 min in PBS, then 2 x 5 min in TBST. After the washing, the membranes were blocked in 5% nonfat dried milk in TBST for another hour, then incubated with the next primary antibody.

Table 31: Abcam stripping buffer

Stripping buffer
15 g/l Glycine
1 g/l SDS
10 ml/l Tween20
pH = 2.2

2.6 Cell viability, growth, migration and invasion

2.6.1 Clonogenic assay

To determine the capacity of the cells to form colonies, clonogenic assays were performed. For this 10^3 cells were seeded in a 24-well plate and grown over night. After about 24 h, cells were treated with growth factors and/or inhibitors (no

treatment in case of the transgenic cells) and allowed to grow for 7-14 days, depending on their growth speed. After 7-14 days, the cells were washed with PBS, fixed with a methanol-acetic acid mixture (3:1) for 20 min and again washed with PBS. Then the cells were stained with crystal violet (10% CV in ethanol, 1:1000 in PBS) for 1-3 h. To remove the excessive crystal violet, the plates were washed carefully with ddH$_2$O and air-dried over night.

Pictures of the stained colonies were taken with a Nikon D90 camera, and afterwards the cells were destained with 2% SDS for about 3 h. The solution was transferred into a 1.5 ml tube and vortexed. Then 100 µl of the solution were pipetted into a microtiter 96-well plate (in duplicates or triplicates) and the absorption at 562 nm was photometrically measured with a SynergyHT plate reader (BioTEK).

2.6.2 MTT assay

The viability of cells was evaluated by MTT assays (MTT kit EZ4U, Biomedica Austria). This colorimetric assay is based on the reduction of the tetrazolium dye MTT (3-(4,5-Dimethylthiazol-2-yl)-2,5-diphenyl-tetrazolium bromide) to the orange colored formazan derivative by mitochondrial enzymes. Since mitochondria are inactivated after cell death within a few minutes, only viable cells with active and functional enzymes lead to the production of the derivative, therefore the coloration reflects the number of viable cells.

2 x 10^3 cells were seeded in 100 µl medium containing 10% serum in 96-well plates and were allowed to recover over night. On the next day treatment was added; or in case of the transgenic cells only the medium was changed to a medium containing only 0.1% serum. After the treatment, respectively the medium change, the cells were allowed to grow for another 3-5 days. Then the medium was aspirated and 100 µl fresh medium with 10% EZ4U reagent were added to the wells. 100 µl of the mixture in empty wells were taken as a blank.

After 1-3 h at 37°C the absorbance at 450 nm was measured. Also the reference absorbance at 620 nm was measured to correct for nonspecific background values.

2.6.3 Platypus migration assay

For investigating the migration behavior of treated as well as transgenic cell lines, a platypus migration assay was performed. For this, the Oris Cell Migration Assembly Kit was used.

The 96-well plate was populated with stoppers and 2 x 10^4 cells were seeded in 100 µl medium into each well with a stopper. The cells were then allowed to attach and grow for 1-2 days. After the cells attached properly, the stoppers were removed and the wells were washed twice with PBS to remove unattached cells. Then 200 µl medium and treatment (no treatment in case of the transgenic cell lines) were added (t = 0). As control, cells grown under the same circumstances but without treatment were used. Pictures were taken regularly, for example after 4, 8, 24, 28, 32, 48 and 52 h.

To non-flourescent cells, cell tracker green (Invitrogen, final concentration: 2 μM) was added 1 h before removing the stoppers. Cells expressing fluorescent proteins were not treated with cell tracker.

To elicit the different migration behavior, the percentage of the covered and the empty area were measured with ImageJ (see figure 11).
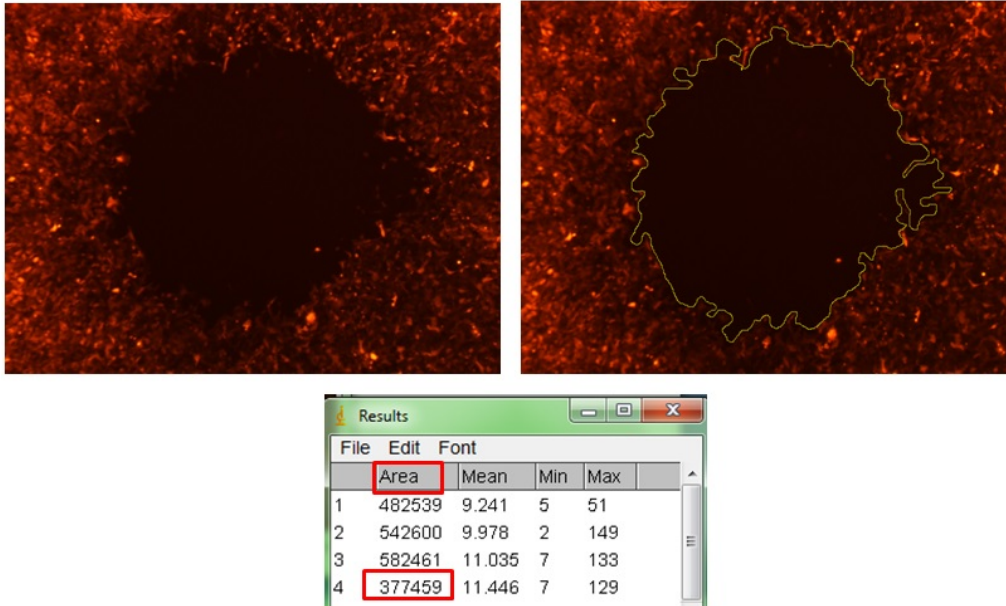
Figure 11: Analysis of the pictures of the platypus assay, measuring the empty area.

2.6.4 Transwell migration assay

For analyzing the capability of the different transgenic cell lines to transmigrate, a transwell migration assay using BD Falcon cell culture inserts with 8 μm pore size in the 24-well format was performed.

4×10^4 cells in 200 μl medium containing 10% serum were seeded into a transwell chamber (BD Falcon). The chambers were put into the wells of a 24-well plate containing 800 μl medium (also with 10% serum). The cells were allowed to transmigrate for 24 h. On the next day, the chambers and the medium in the wells were removed, the cells which had transmigrated and attached to the bottom of the well were washed with PBS and 1 ml fresh medium containing 10% serum was added. The cells were then allowed to grow for another 7-10 days, after which they were further handled like cells for the clonogenic assay.

Meanwhile the chambers were transferred into a new 24-well plate, where they were washed with PBS and cells still sitting inside the chamber were removed. Then the cells which had transmigrated to the lower surface of the chamber but did not fall off were fixed by adding ice-cold MetOH and putting them at -20°C for 20 min. After that the chambers were again washed with PBS and the cells were stained with crystal violet for about 4 h. After pictures of the bottom

side were taken, the cells were destained with 2% SDS for about 3 h, then the absorbance of the solution was measured at 562 nm like for the clonogenic assay.

2.6.5 Spheroid formation assay

For the spheroid formation assay, 5 x 10^3 cells were seeded in a low attachment 24-well plate in 1 ml DMEM/F12 medium supplemented with B-27 Serum-Free Supplement (Life technologies). Additionally FGF2 (20 ng/ml) and EGF (20 ng/ml) or only EGF (also 20 ng/ml) were added, to check whether the FGF2 overexpressing cell lines could compensate the lack of FGF2 in the medium.
For the evaluation of the spheroid forming capability, pictures were taken after 3, 7 and 10 days. The diameters of the spheres were measured with ImageJ, the mean radius and the volume were calculated in MS Excel. To analyse the overall sphere volume, the number of spheres and the average volume of each sphere, respectively of only the large spheres with a mean radius over 50μm, an R-script was developed with the help of Sascha Wiplinger. The calculated radius and volume of each sphere were put into a data.frame, the odd columns containing the radius, the even columns containing the volume.

R - Version 3.1.0, "Spring Dance"; released 10.04.2014; Platform: x86_64-pc-linux-gnu (64-bit).

```
#input_file data: path to csv file with following format:
    type_well1_radii | type_well1_volumes | ... | type_
    welln_radii | type_welln_volumes

sphere_summary <- function(input_file, output_file) {

        data <- read.csv2(input_file)
        columns <- ncol(data)
        rows <- nrow(data)

        summary <- data.frame(number_of_spheres=numeric(
            columns/2), avg_volumes=numeric(columns/2), sum
            _volumes=numeric(columns/2), number_of_spheres_
            gt_50=numeric(columns/2), avg_volumes_gt_50=
            numeric(columns/2), sum_volumes_gt_50=numeric(
            columns/2),stringsAsFactors = FALSE)

        col_names = c('#_of_spheres', 'Avg._volume', 'Sum_
            of_volumes', '#_of_spheres_>=_50', 'Avg._volume
            _>=_50', 'Sum_of_volumes_>=_50')
        row_names <- vector()
        radi_col <- vector()
```

```r
for (column in 1:columns) {
        col <- data[, column]
        col <- col[!is.na(col)]

        if(column %% 2 == 0) {  #if volumes, do
            calculations###########################
        mean_total <- mean(col)
        mean_gt_50 <- mean(col[radi_col >= 50])
        sum_total <- sum(col)
        sum_gt_50 <- sum(col[radi_col >= 50])
        spheres_total <- length(col)
        spheres_gt_50 <- length(col[radi_col >=
            50])

        # add calculated stuff as new row to
            summary
        new_line <- c(spheres_total, mean_total,
            sum_total, spheres_gt_50, mean_gt_50,
            sum_gt_50)
        summary[column/2, ] = new_line
        #print( gsub(”_volumen$”, ””, colnames(
            data[column])))
        row_names <- c(row_names, gsub(”_volumen$”
            , ””, colnames(data[column])))
        }
        else {  # if radii, save column for
            further calculations############
                radi_col <- col
        }
}

colnames(summary) <- col_names
row.names(summary) <- row_names
write.csv2(summary, output_file)
return(summary)
}
```

2.7 Statistical analysis

The experiments were performed at least in triplicates, unless stated otherwise.
Resulting data are presented as means and standard deviation of the replicates.
Statistical significance was analyzed using GraphPad Prism 5.0 software (Graph-
Pad Software Inc.). A p-value equal or below 0.05 was considered statistically

significant (*), p-values from 0.01 to 0.001 as very significant (**) and p-values below 0.001 as highly significant (***).

3 Results

3.1 Morphology and behavioral changes upon treatment with growth factors and/or inhibitors in MPM cell lines

3.1.1 Morphology changes

Only the biphasic SPC212 and M38K cell lines change their morphology upon treatment with FGF2

Since the two biphasic MPM cell lines M38K and SPC212 change their morphology to a more fibroblastoid phenotype upon treatment with FGF2, various other MPM cell lines like the biphasic SPC111, the epithelioid p31 and VMC20 as well as the sarcomatoid Meso62 and Meso80 were treated under the same conditions with FGF2. None of the cell lines showed morphology changes (for the changes in the SPC212 cell line see figure 12, data of the M38K shown below, data of other cell lines not shown).
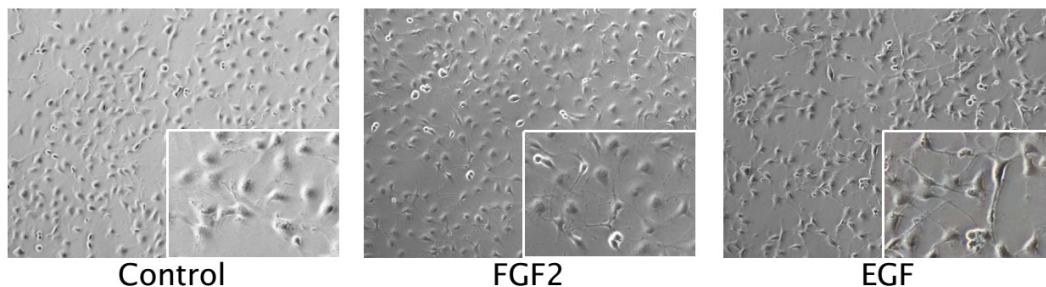
Figure 12: Morphology changes in the SPC212 cell line upon treatment with FGF2 and EGF for 24 h.

Only FGF2 and EGF induce morphology changes in the biphasic MPM cell lines SPC212 and M38K

To determine the growth factor specificity of the morphology changes, M38K cells were treated with various FGFs, namely FGF1, 5 and 18, and other growth factors known to induce EMT or at least morphology changes in other cell lines. Treatment with other FGFs however did not induce morphology changes in the M38K cell line, neither did treatment with HGF, PDGF, TGF-β, BMP2 or Activin A. Only EGF induces changes similar to the ones induced by FGF2 treatment (see figure 13 and figure 14).
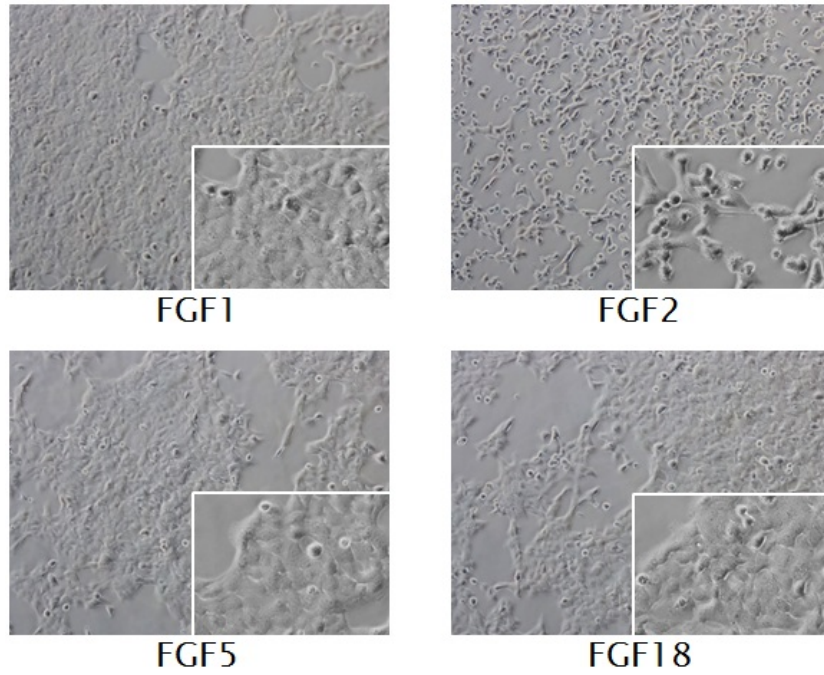
Figure 13: Treatment with other FGFs for 24 h does not induce any changes similar to those induced by FGF2.
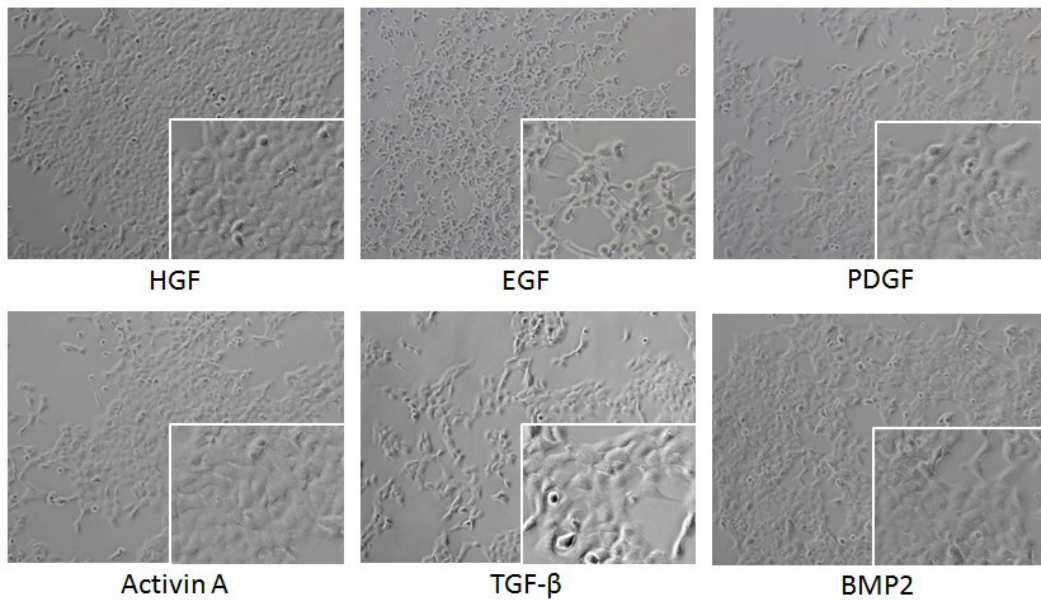
Figure 14: Morphology changes in M38K cells upon treatment with other growth factors for 24 h; only EGF induced similar morphology changes.

A short exposure to FGF2 is enough to induce morphology changes
To answer the question how long the cells need to be stimulated by FGF2 treatment to change their morphology, cells were treated for one minute and for five

minutes, after which FGF2 was removed. Pictures were then taken after 24 h. Even after the short treatment for only one minute, M38K cells showed the characteristic morphology changes, which were persistant for about 48 h (see figure 15).
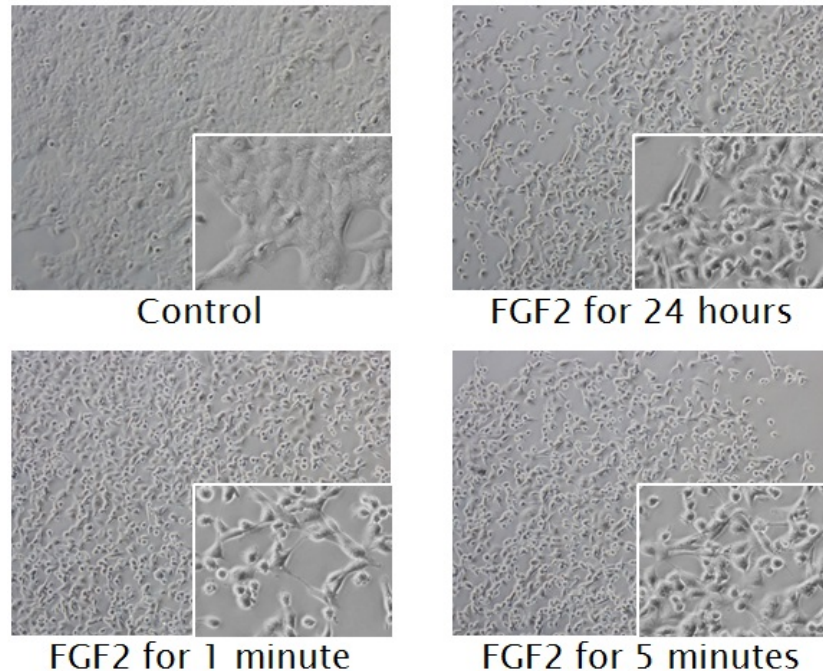
Figure 15: M38K cells show similar effects after treatment with FGF2 for either 24 h, one minute or five minutes. Images were taken 24 h after treatment start.

Receptors for other growth factors are expressed but do not stimulate morphology changes

Since the other tested growth factors are known to induce changes in other cell lines, the lack of morphology changes upon growth factor treatment suggested a lack of the respective receptors. But according to the whole genome gene expression microarray data of M38K cell lines, receptors for all tested growth factors are expressed in the cell line, at least on transcript level (see figure 16).
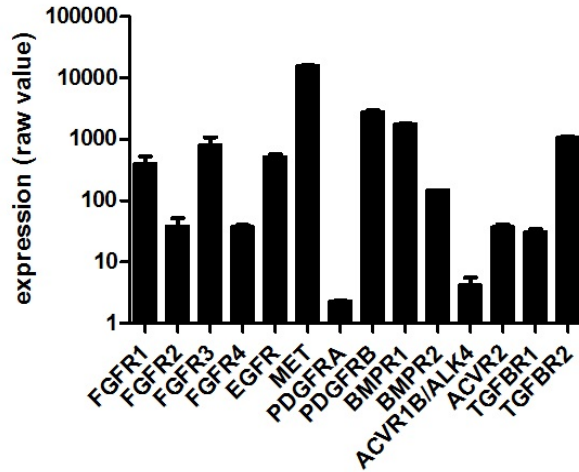
Figure 16: Transcript expression levels of the receptors for the tested growth factors in the M38K cell line.

The visible effects of FGF2 were the same in M38K cells kept in medium with 10% FCS and in serum-free medium

Since some cells are known to undergo growth factor-induced morphology changes only under serum-deprived conditions, the serum-requirement of the M38K cells was determined. The cells were starved for 24 h before and during the treatment with the various growth factors. But also under these conditions the effects were the same as in full serum - only FGF2 and EGF induced the morphology changes (see figure 17 and figure 18).
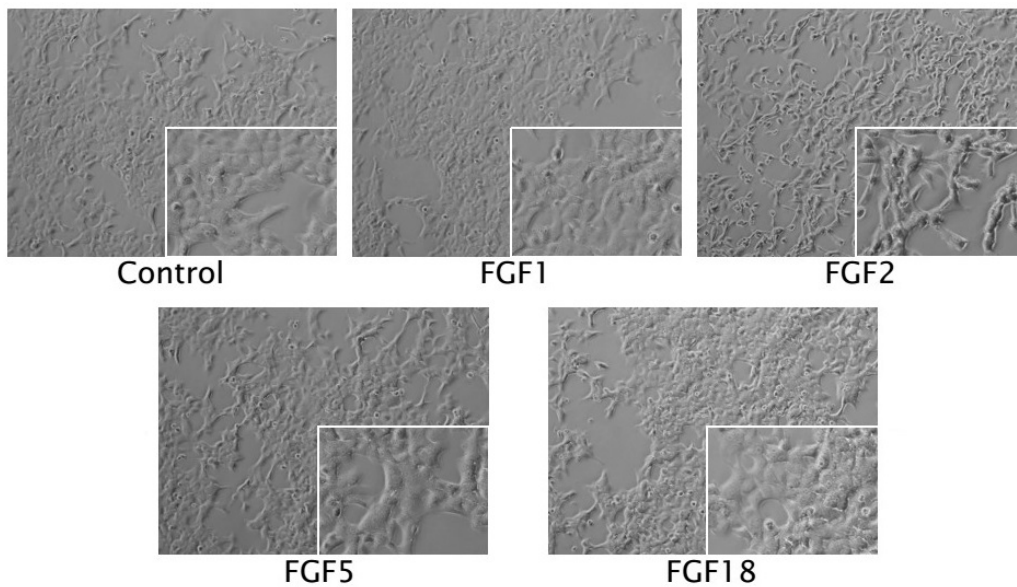
Figure 17: Morphology changes in serum-starved M38K cells following treatment with various FGFs for 24 h, only FGF2 induced changes.
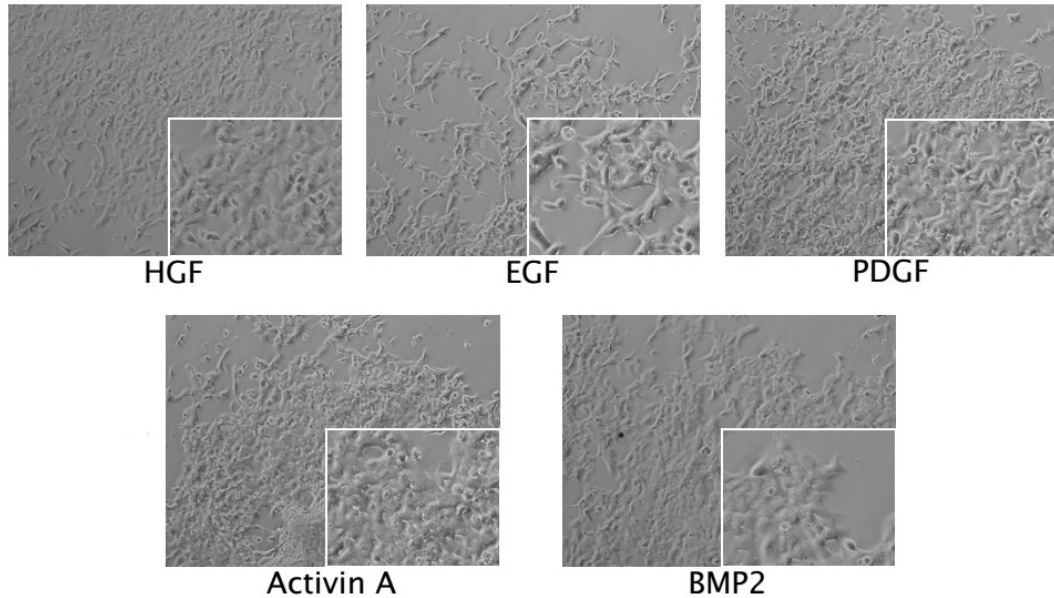
Figure 18: Morphology changes in serum-starved M38K cells following treatment with other growth factors for 24 h, only EGF induced similar morphology changes.

The MEK-pathway is necessary for the FGF2-induced changes

To determine which of the several RTK-stimulated signaling pathways is required for the observed changes upon treatment with FGF2, co-treatment with FGF2 and inhibitors of various downstream signaling proteins was tested in the M38K cells. The inhibitors UO126 and selumetinib (both MEK inhibitors), ponatinib (inhibits multiple tyrosine kinases including FGFRs) and PD166866 (inhibits the tyrosine kinase domain of FGFR1) inhibited the changes when co-treated with FGF2, whereas other inhibitors such as LY294002 (PI3-kinase inhibitor), SB431542 (TGF-β and activin receptor inhibitor) and MK2206 (AKT inhibitor) could not prevent the changes. The finding that MEK inhibitors can prevent the morphology changes indicate that the MEK-pathway is the one necessary for the signal transduction, not the PI3K pathway involving Akt (see figure 19).
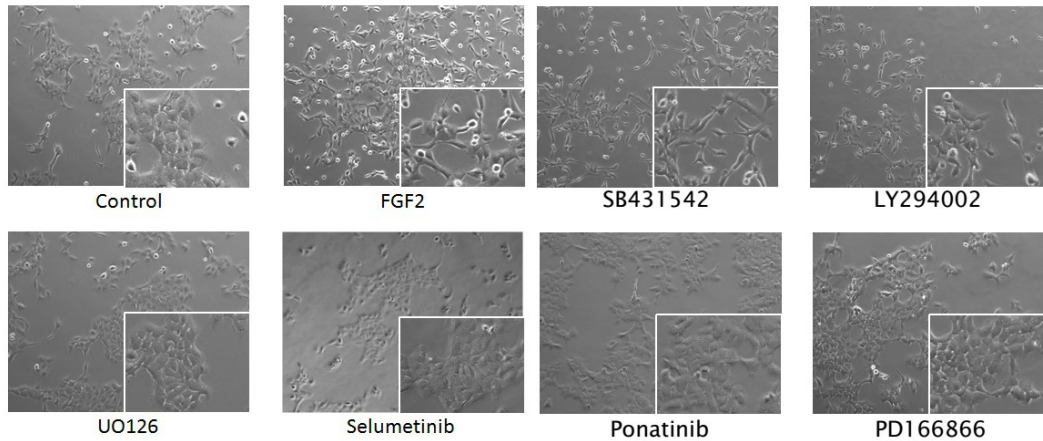
Figure 19: Co-treatment with FGF2 and one of the inhibitors UO126, pona-
tinib, PD166866 and selumetinib prevented the morphology changes,
whereas LY294002, SB431542 and MK2206 did not prevent the
changes (data of MK2206 not shown).

3.1.1.1 Quantification of the morphology changes

**The FGF2-induced morphology changes were significant in FGF2-
treated cells**

Since FGF2 and partially also EGF not only induced morphology changes but
also scattering of the M38K cells, the effect can be quantified by counting the
contiguous cell clusters as a measure of the extent of scattering. In cells treated
with FGF2 a significantly higher number of cell clusters can be seen, whereas
other growth factors did not or only weakly induce scattering in the cells. Also
in serum-starved cells the effects induced by FGF2 are significant (see figure 20).
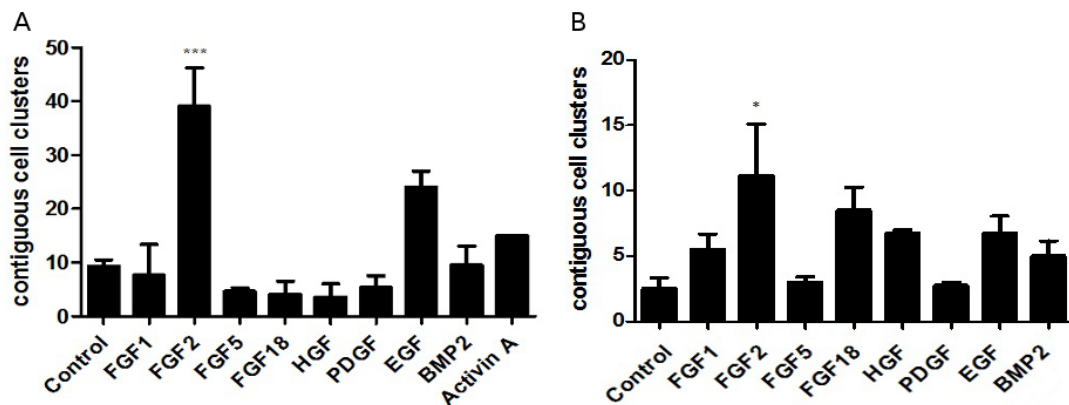
Figure 20: A significantly higher number of contiguous cell clusters in M38K
treated with FGF2 in full serum (A) and in starved cells (B). Here,
only one image of Activin A treated cells was evaluated, of the other
treatments 3-6 pictures each were evaluated.

With this quantification method it could also clearly be seen that the inhibitors ponatinib, PD166866 and UO126 can prevent the scattering of the cells almost to the level of the control without any treatment. The other inhibitors showed no or less inhibition of the scattering compared to the FGF2 control (see figure 21).
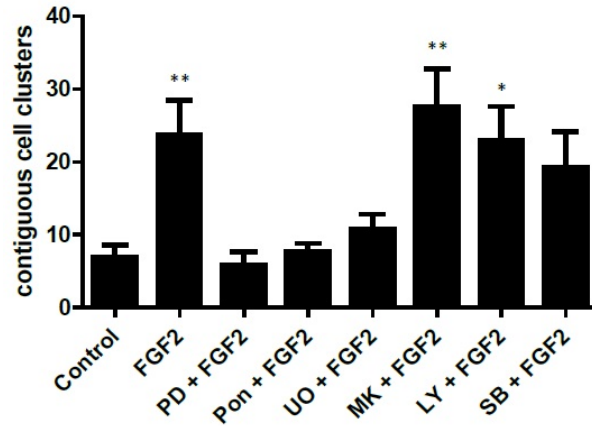
Figure 21: Quantification of the effects in the M38K cell line when treated with various inhibitors.

M38K cells treated with FGF2 lose contact to other cells

Another way to quantify the morphology changes is to measure the cell-cell contact of the cells. In figure 22 it can be seen that treatment with FGF2 highly reduces the percentage of cell-cell contact compared to the non-treated control. The inhibitors UO126 and PD166866 prevent the loss of cell-cell contact upon treatment with FGF2.
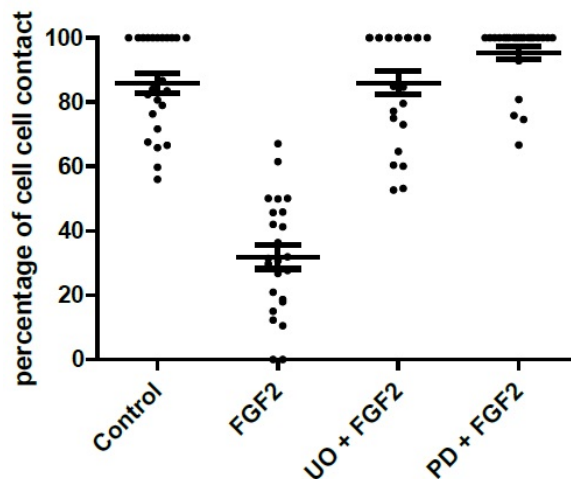
Figure 22: Quantification via measurement of cell cell contact.

3.1.2 Changes in the migration behavior upon treatment with growth factors and/or inhibitors

FGF2 increases the migration behavior in the biphasic cell lines M38K and SPC212

The morphology changes and the scattering of the cells upon treatment with FGF2 suggest EMT in those cells, which normally also involves an increase of migration. To test this, a platypus migration assay was performed with the two cell lines. FGF2 stimulated migration, whereas UO126 decreased cell migration below the basal level of the control in the M38K cells. This indicates that the cells have a basal, external FGF2-independent migration which requires the MEK-pathway. The migration induced by FGF2 could not be completely inhibited by UO126, suggesting another pathway involved in the stimulation of migration. FGF2 also slightly increased the migration in the SPC212 cell line, the influence of UO126 on this cell line was not tested (see figure 23).
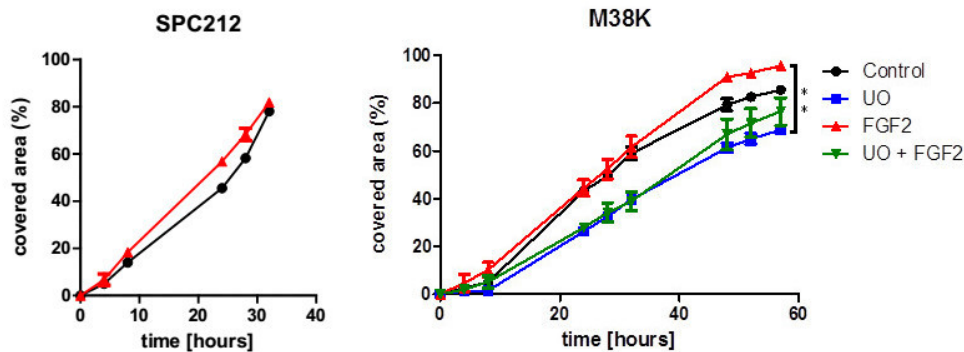
Figure 23: Treatment with FGF2 increases the migration of the M38K cells, whereas treatment with UO126 decreases it.

3.1.3 Changes in the signaling pathways

FGF2 treatment stimulates the phosphorylation of ERK

To confirm the findings regarding the involved signaling pathway upon FGF2 stimulation, the phosphorylation status of various downstream proteins was checked in the biphasic cell line M38K. Upon treatment with FGF2 for 15 min the phosphorylation level of ERK increased, whereas there was no detectable phosphorylation of PLC-γ1 or S6. Co-treatment with one of the inhibitors UO126, ponatinib or PD166866 could prevent the signaling and therefore the ERK-phosphorylation, whereas the other inhibitors did not prevent the phosphorylation upon FGF2 treatment (see figure 24).
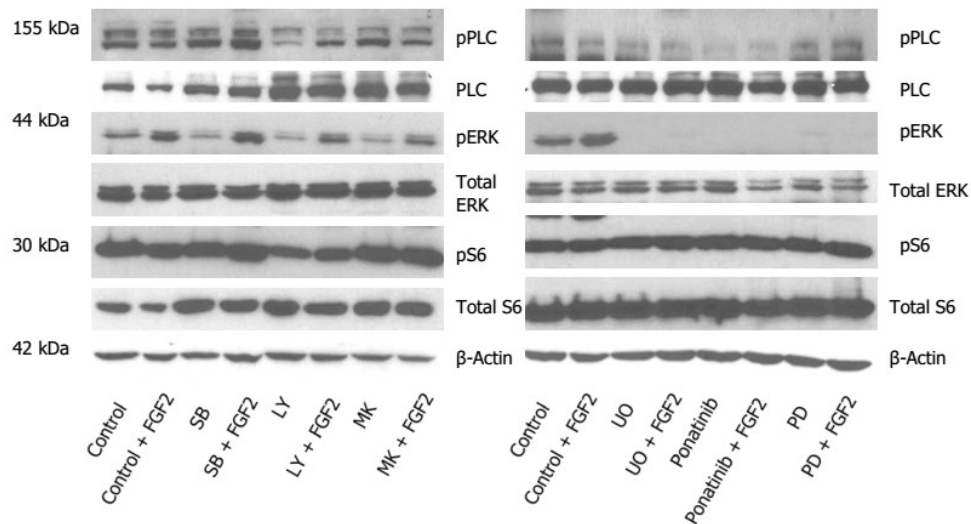
Figure 24: Phosphorylation of ERK is increased upon treatment with FGF2, except when co-treated with PD166866, ponatinib or UO126.

FGF2-induced phosphorylation of ERK also occurs in cell lines not undergoing morphology changes

To determine if cell lines which did not show any phenotypic changes upon FGF2 treatment show differences in the signaling pathway, the phosphorylation status of ERK and AKT was analysed. The FGF2-induced ERK-phosphorylation was seen in the biphasic cell line SPC212, the epithelioid cell lines VMC20 and p31, as well as in the sarcomatoid cell line Meso62. Co-treatment with the MEK inhibitor selumetinib prevented the phosphorylation of ERK in all tested cell lines (see figure 25).

Comparison of the cell lines showed different basic pERK level in the cell lines

Since the fibroblast-like morphology and the increased migration in the biphasic cell lines M38K and SPC212 upon FGF2 treatment reminds one of the sarcomatoid histotype, a constant stimulation of the MEK-pathway in sarcomatoid cell lines was hypothesized. This would mean a higher basic phosphorylation level of ERK, without FGF2 treatment. The two sarcomatoid cell lines Meso62 and Meso80 do indeed have a higher basic phosphorylation lavel of ERK, but so does the epithelioid cell line p31 (see figure 26).
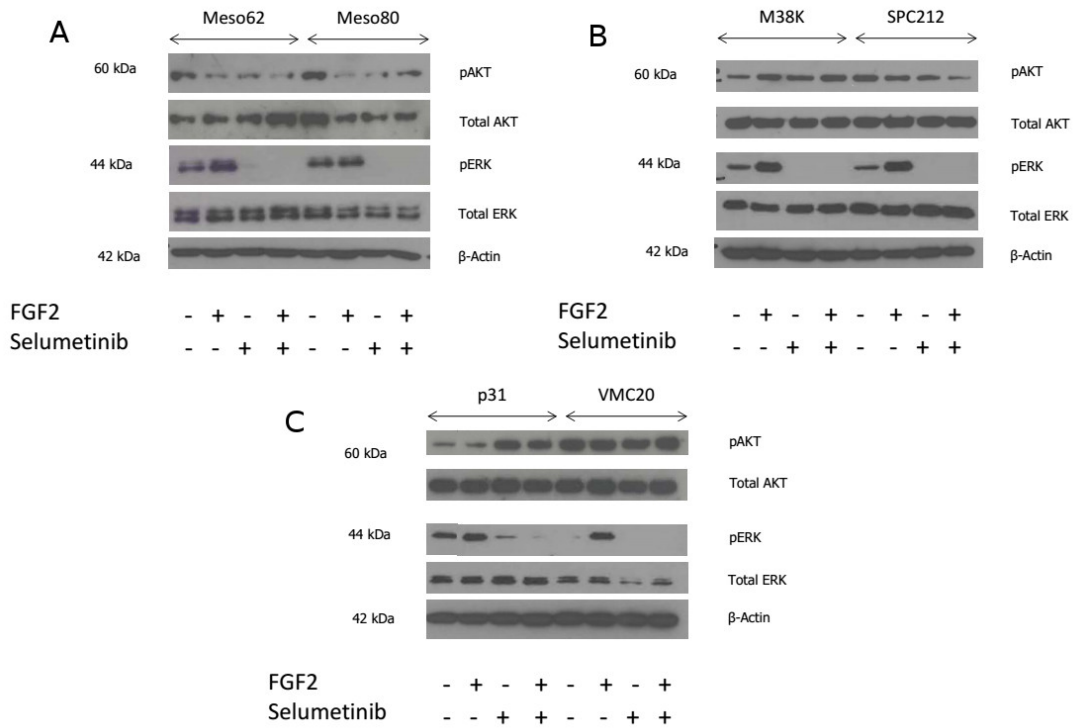
Figure 25: Increase of the pERK level in all tested cell lines except Meso80; selumetinib inhibits the phosphorylation in all cell lines. A: sarcomatoid cell lines. B: biphasic cell lines. C: epithelioid cell lines.
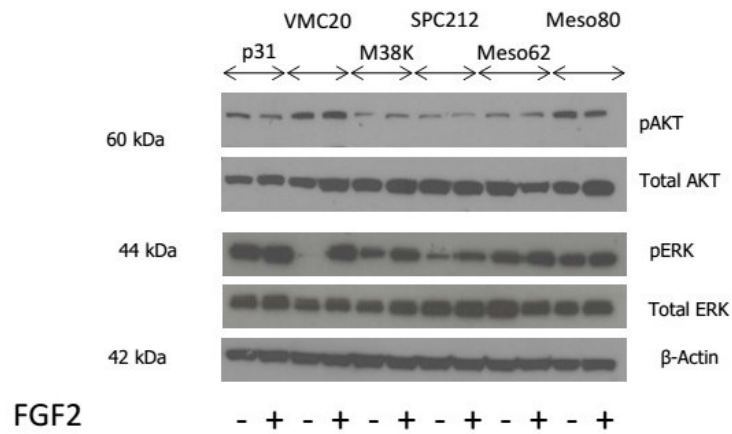
Figure 26: Meso62, Meso80 and p31 have a higher basic pERK level.

3.1.4 Changes in the colony-forming capabilities and the viability upon treatment with selumetinib

Treatment with selumetinib limits the colony-forming capabilities of MPM cell lines

To determine whether the sarcomatiod cell lines, which have a higher basic pERK level and show a more fibroblast-like morphology *a priori*, are more sensitive to inhibition of the MEK-pathway, which is responsible for the changes in the biphasic cell lines, the colony formation of MPM cell lines upon prolonged treatment with selumetinib was determined using clonogenic assays. The treatment of the various MPM cell lines in various concentrations showed, that the epithelioid cell line p31, the biphasic cell lines SPC212 and M38K and - although not as prominent as in the other cell lines - the sarcomatoid cell line Meso62 are sensitive to treatment with selumetinib, regarding their colony-forming capabilities. The epithelioid cell line VMC20 shows a decrease only at the concentration of 10 µM, whereas the sarcomatoid cell line Meso80 shows no effect at the highest concentration whereas 0.1 µM and 1 µM seem to induce a slight decrease (see figure 27).
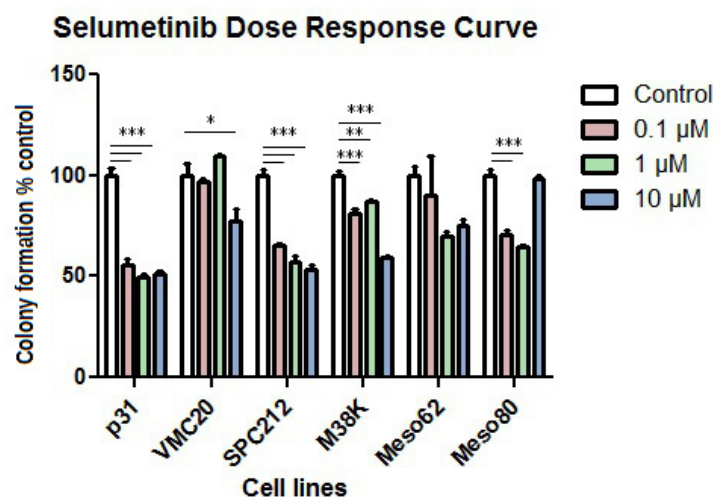
Figure 27: Treatment with selumetinib decreased colony formation in p31, M38K, SPC212 and Meso62 cell lines (not significant in Meso62).

Selumetinib decreases the viability of sarcomatoid MPM cell lines

To test whether selumetinib also decreases the viability of the sarcomatoid cell lines, MTT assays were performed. The sarcomatoid cell line Meso62, as well as the biphasic cell line M38K show a reduced viability upon treatment with selumetinib at a concentration of 2000 nM, the sarcomatoid cell line Meso84 shows a decrease already at 500 nM (see figure 28).
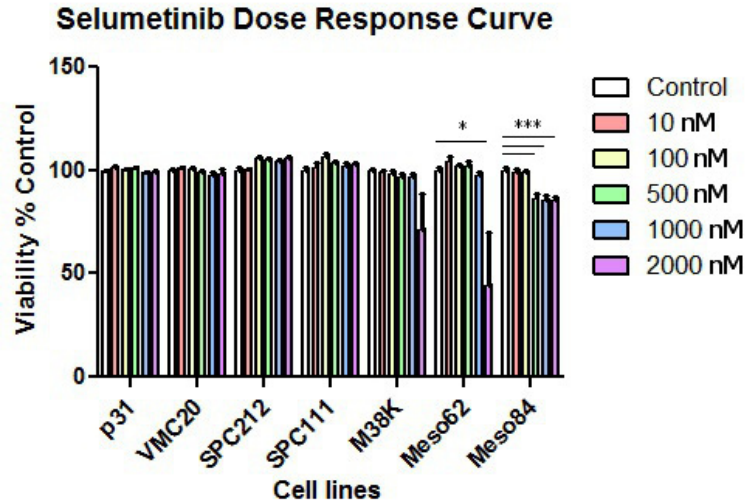
Figure 28: Treatment with selumetinib decreased viability in the sarcomatoid
Meso62 and Meso84 cell lines, as well as in the biphasic cell line M38K
(although not significantly).

3.2 Morphology changes upon treatment with growth factors in other cell lines

3.2.1 HT29 and DLD-1

Treatment conditions inducing morphology changes in MPM cell lines do not induce changes in cell lines known to undergo EMT upon EGF/FGF2 treatment

Since it was shown that prolonged treatment with FGF2 and/or EGF induces morphology changes and EMT in the two colon carcinoma cell lines HT29 and DLD-1 in serum-deprived medium, a treatment similar to the MPM cell lines was tested (FGF2 or EGF alone: concentration = 10 ng/ml; FGF2 and EGF together: FGF2 - 10 ng/ml, EGF - 20 ng/ml; in medium containing 10% serum). After 24 h no morphology changes were visible. After 6 days however, small changes were visible in the DLD-1 cells treated with FGF2 and EGF (see figure 29). In the HT29 no changes were seen, neither after 24 h nor after 6 days. On the contrary, co-treatment with FGF2 and EGF caused the HT29 cells to die more rapidly (images not shown).
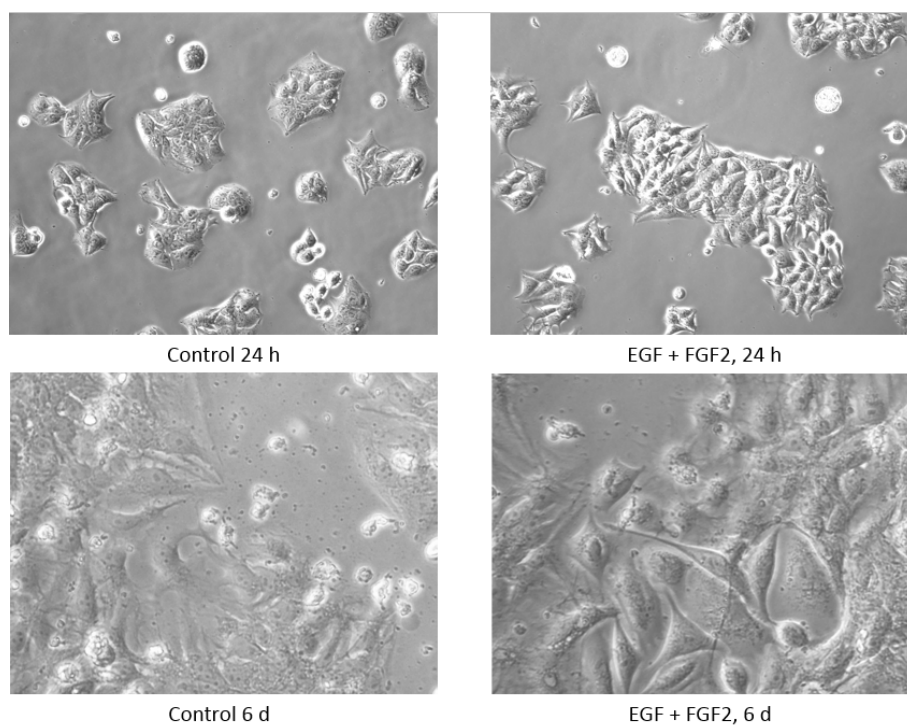
Figure 29: DLD-1 cells show no morphology changes after 24 h, and only small changes after 6 days. For a better visibility the images from day 6 show a higher magnification.

Also treatment with other growth factors did not induce changes in the colon carcinoma cell lines

Given that FGF2 and EGF treatment did not induce strong changes in the DLD-1 cell line and none in the HT29 cells under the conditions described above, other growth factors were also tested on these cells. But also PDFG and Activin A did not induce any changes. HGF (also 10 ng/ml) however caused stress in both cell lines and rapid death (see figure 30).

Under serum-starving conditions morphology changes were induced

In the original experiment the DLD-1 and HT29 cells were kept in serum-deprived medium to induce the EMT-like changes [43]. To determine if the cells react to the growth factors under starving conditions, medium of the cells was changed to serum-free medium before treatment. Treatment was applied as described before. The HT29 showed slight changes after 48 h but rapidly died after this time. Many of the DLD-1 cells died upon the starvation at first, but the surviving cells showed morphology changes after 6 days (see figure 31).
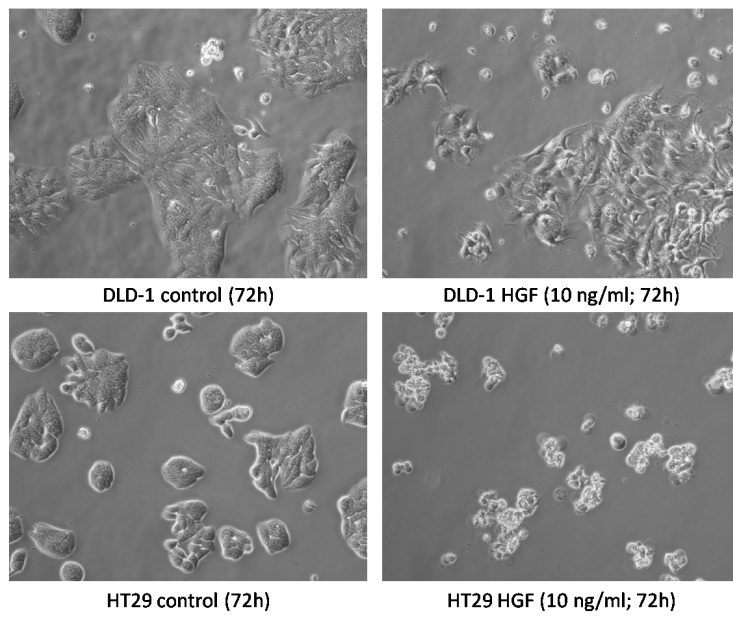
Figure 30: HGF induces stress and cell death in DLD-1 and HT29 cells after 72 h.
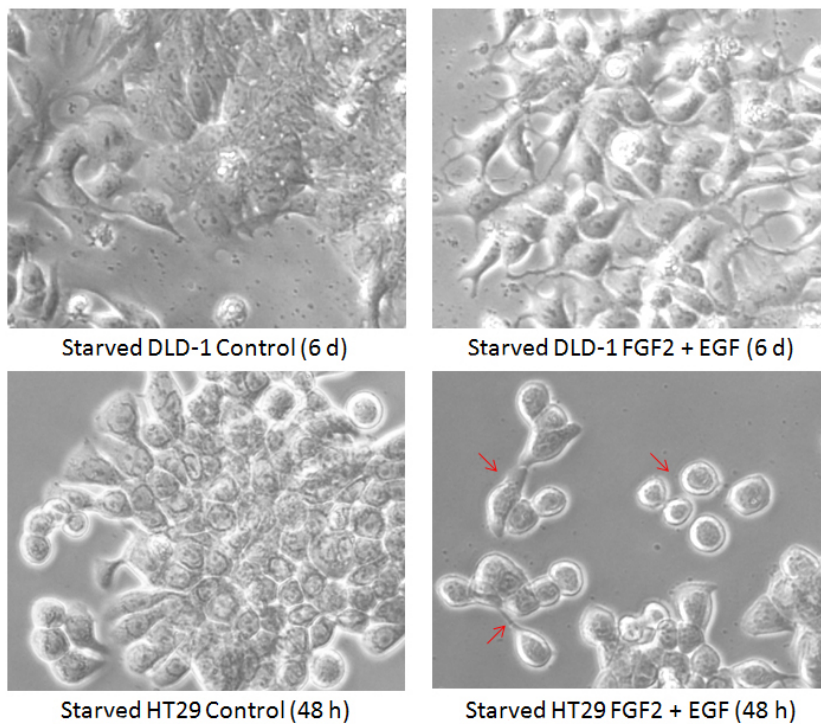
Figure 31: Morphology changes in the HT29 and DLD-1 after 48 h respectively 6 days. HT29 only slightly scatter and elongate upon the treatment (red arrows).

3.2.2 HepG2 cells

Treatment of HepG2 cells with EGF and FGF2 did not induce morphology changes
Since HepG2 cells are known to show morphology changes, scatter and undergo EMT upon treatment with HGF, they were also treated with EGF, FGF2 and as a control, HGF. Treatment with EGF and/or FGF2 however did not induce any changes even after 6 days, whereas the treatment with HGF induced a more fibroblastoid shape after 24 h (see figure 32).

HepG2 Control (24 h)   HepG2 FGF2 + EGF (24 h)   HepG2 HGF (24 h)
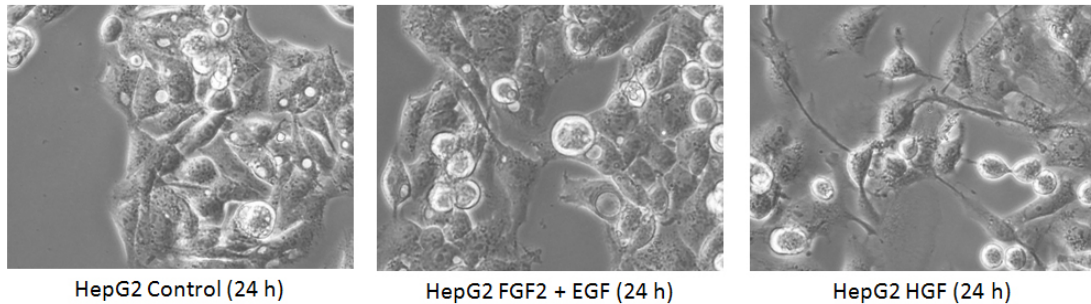
Figure 32: Morphology changes in the HepG2 cell line upon treatment with HGF.

3.3 Transgenic cell lines

3.3.1 Expression of the transgenes

Retrovirally transduced M38K and SPC212 show a exceedingly high expression level of the respective transgene
To determine whether overexpression of FGF2 induces changes comparable to the ones induced by FGF2 treatment in the M38K and SPC212 cells, transgenic cell lines overexpressing FGF2 were established. Since array data of M38K cells also showed high expression levels of FGF18, also FGF18 overexpressing cell lines were created. The expression of the FGF2 and FGF18 transgenes in the retrovirally transduced cell lines was verified by TaqMan qPCR. The $2^{-\Delta\Delta Ct}$ values of the expression on the RNA level can be seen in figure 33. All cell lines clearly overexpress the transduced genes.
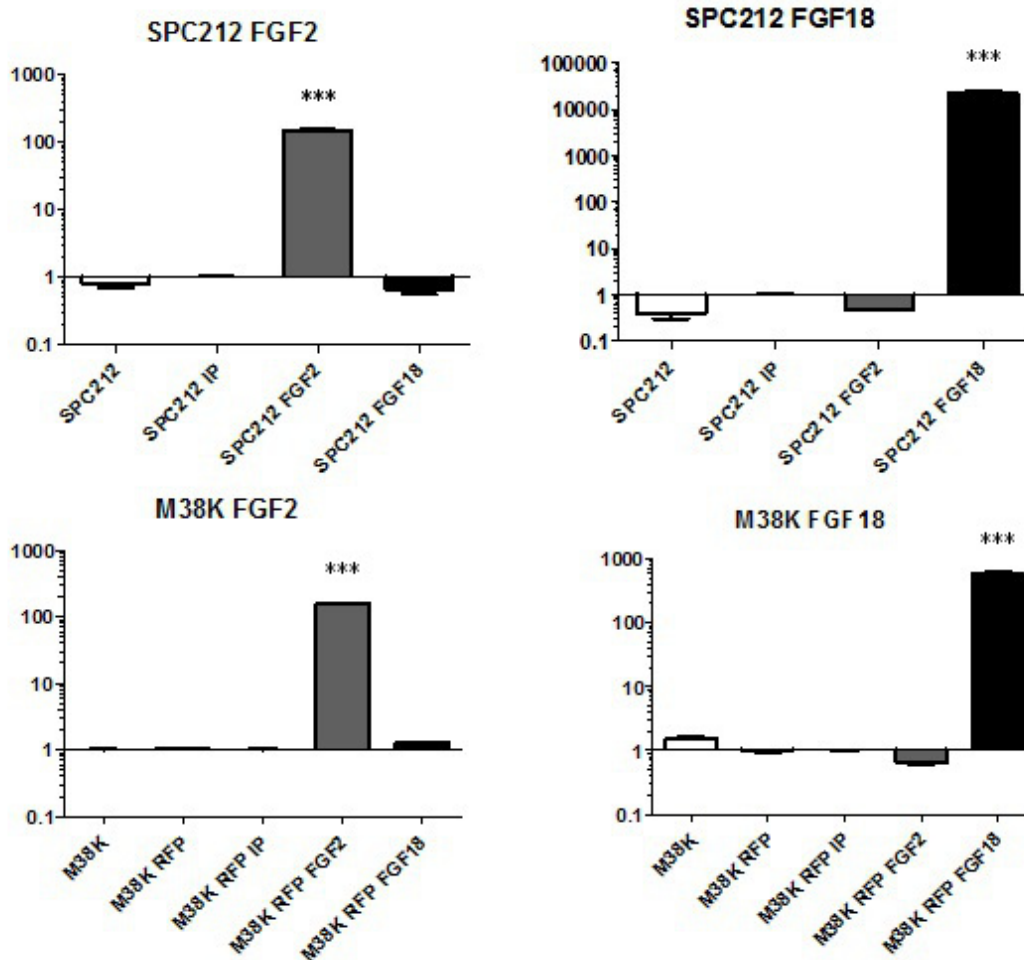
Figure 33: The $2^{-\Delta\Delta Ct}$ values of the expression on the RNA level. For comparison the parental SPC212 and M38K cells and cell lines carrying an empty vector (IP, IresPuro) were used. The M38K cell lines additionally express a red fluorescent protein (RFP).

3.3.2 Response to external FGF2

Transgenic cell lines still react to external FGF2

The transgenic cell lines overexpressing FGF2 showed no morphology changes, so it was hypothesized that they might have downregulated the receptors due to feedback loops induced by the constant exposure and permanent stimulation. Therefore the transgenic cells were treated with FGF2, which induced the typical morphology changes. This implies that the receptors are still functional (see figure 34).
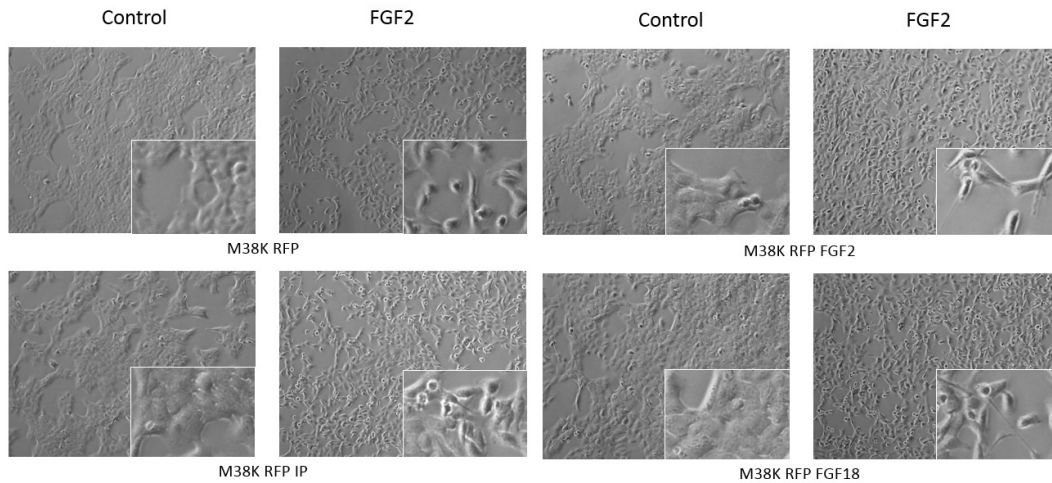
Figure 34: Treatment with FGF2 induces morphology changes also in the transgenic M38K (data of the transgenic SPC212 not shown).

3.3.3 Proliferation and viability

The FGF2 and FGF18 transgenes do not enhance cell proliferation
To determine the influence of the transgenes regarding proliferation of the cells, their colony forming capability was compared to cells carrying an empty (IP, IresPuro) vector and cells without any vector. There is, however, no difference between the transgenic cell lines and the control cell line (see figure 35).
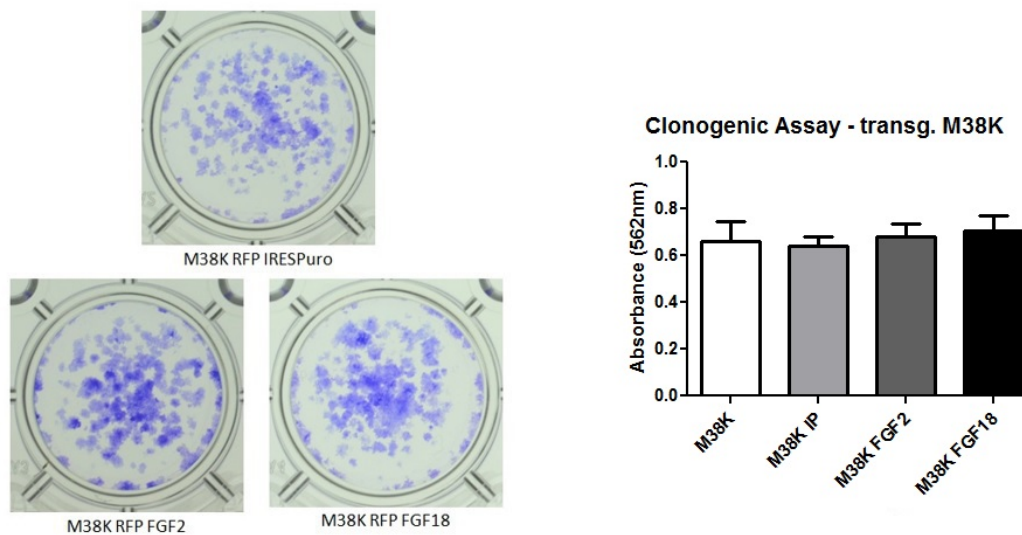
Figure 35: No difference in the colony formation capability of the transgenic cell lines.

In the transgenic SPC212 cells on the other hand, the cells overexpressing

either FGF2 or FGF18 show a lower colony formation capability compared to the IresPuro cells and empty cells (see figure 36; pictures of the wells not shown).
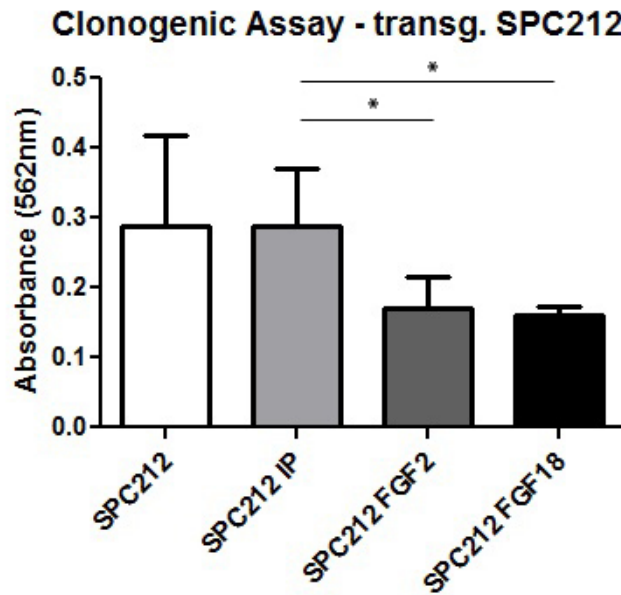
Figure 36: FGF2 and FGF18 overexpressing SPC212 cells show a lower colony formation capability compared to the control.

3.3.4 Differences in the (trans-)migration behavior

The FGF2 transgene increases the migration in the M38K cells
Since exogenous FGF2 clearly increases the migration of the M38K cells, the effects of the FGF2 overexpression regarding the migration behavior were checked. The platypus migration assay shows that the FGF2 transgene in the M38K RFP cell line increases the lateral migration of the cells, compared to the control cell line carrying the empty IresPuro vector and the cell line with the FGF18 transgene (see figure 37).
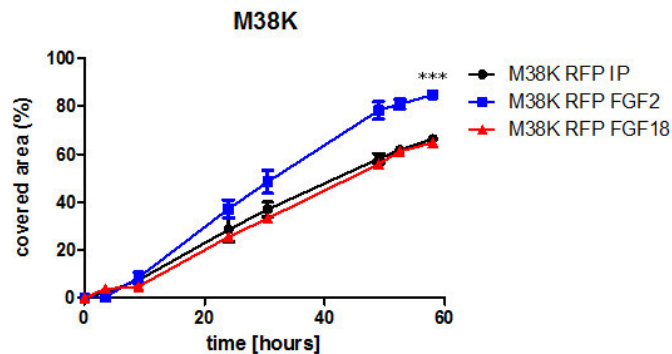
Figure 37: Increase of the migration in the transgenic M38K RFP FGF2 cell line.

The transgenic SPC212 cells show a higher ability to transmigrate compared to the control cell line and the transgenic M38K

To further characterize the behavior of the transgenic cell lines, their ability to transmigrate was tested. The transgenic M38K cell lines did not show a significant difference in their ability to transmigrate through pores and drop into the well below. The SPC212 IP and FGF18 cells however show a higher transmigration rate and drop into the well below, whereas the FGF2 cells transmigrate but rather keep attached to the bottom of the chamber (see figure 38).
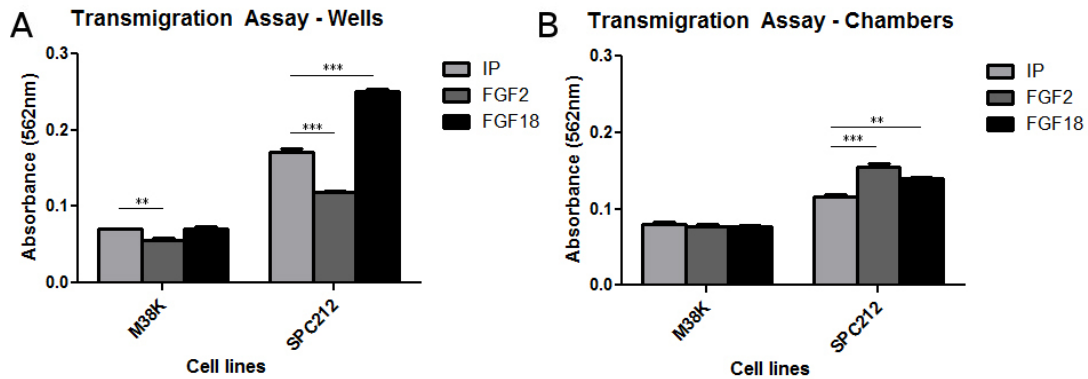
Figure 38: Transgenic SPC212 cells show a higher ability to transmigrate. A: Cells which dropped into the well below. B: Cells which kept attached to the bottom of the chamber.

3.3.5 Spheroid formation capability

The FGF2 overexpressing cells can compensate the missing FGF2 in the medium and form less but larger spheres compared to the control and FGF18 overexpressing cells

To analyze the ability of the transgenic cell lines to form attachment-independent cell aggregates, which should provide an indication of their *in vivo* behavior under non-adhesive conditions, spheroid formation assays were performed. The FGF2 overexpressing M38K formed less but on average bigger spheroids compared to the control (IP) and FGF18 overexpressing cell lines. Additionally the M38K FGF2 cell line could compensate the missing FGF2 in the medium (no significant differences between the groups with and without FGF2), suggesting a sufficient expression and excretion of FGF2 in this cell line (see figure 39, data of the transgenic SPC212 cell lines not shown).
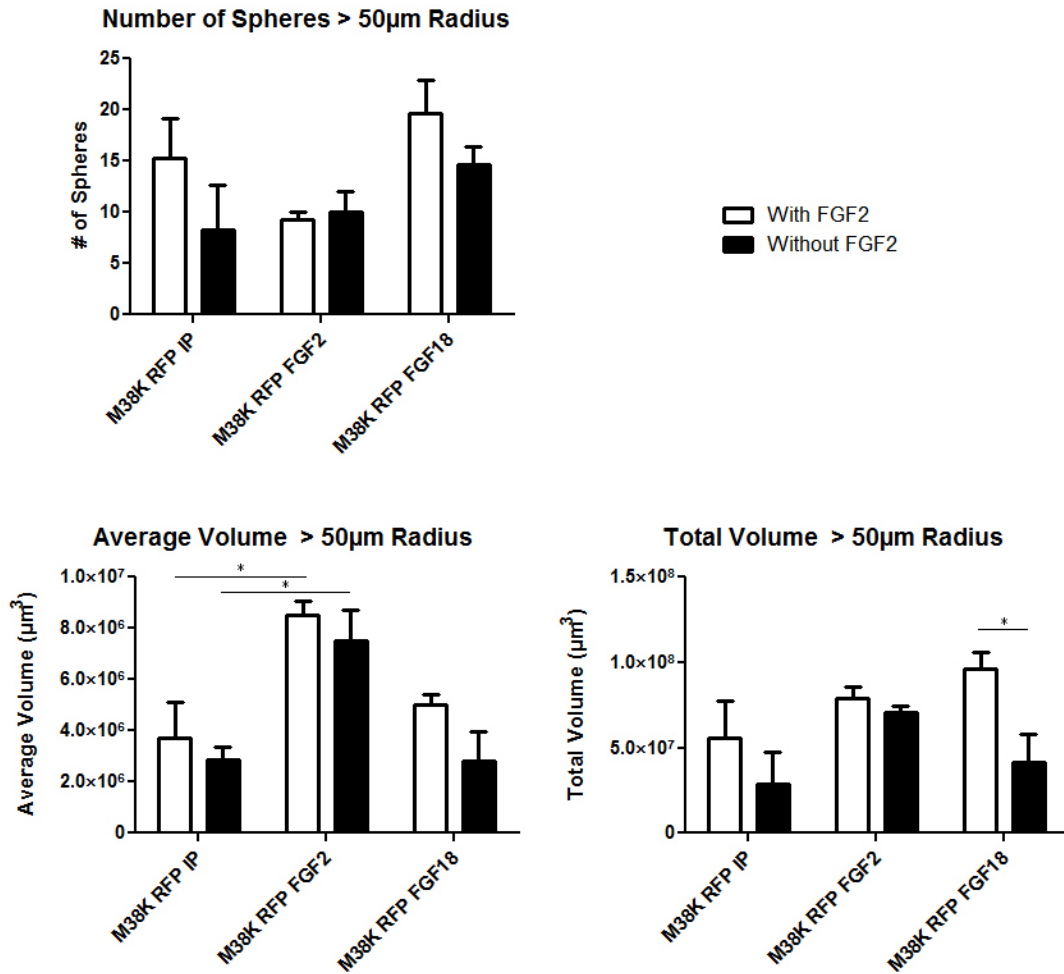
Figure 39: Number, average and total volume of the spheroids with a radius larger than 50 μm formed by the transgenic M38K cell lines with and without FGF2 in the medium. The FGF2 overexpressing cell lines could compensate the missing FGF2 supplementation and formed the on average largest viable spheroids.

3.3.6 Changes in the signaling pathways

The endogenous FGF2 only stimulates the phosphorylation of ERK in the SPC212 cells

Since the treatment with exogenous FGF2 stimulates the phosphorylation of ERK via the MEK-pathway, changes in the phosphorylation status of proteins involved in this pathway were checked in the untreated transgenic cells. In SPC212 FGF2 cells a slighly higher pERK level was seen compared to the SPC212 IP and SPC212 FGF18 cells. In the M38K RFP FGF2 and FGF18 cell lines however, the pERK level did not differ from the one in the control cell line. In both cell lines a higher phosphorylation level of the FGFR-1 was seen (see figure 40).
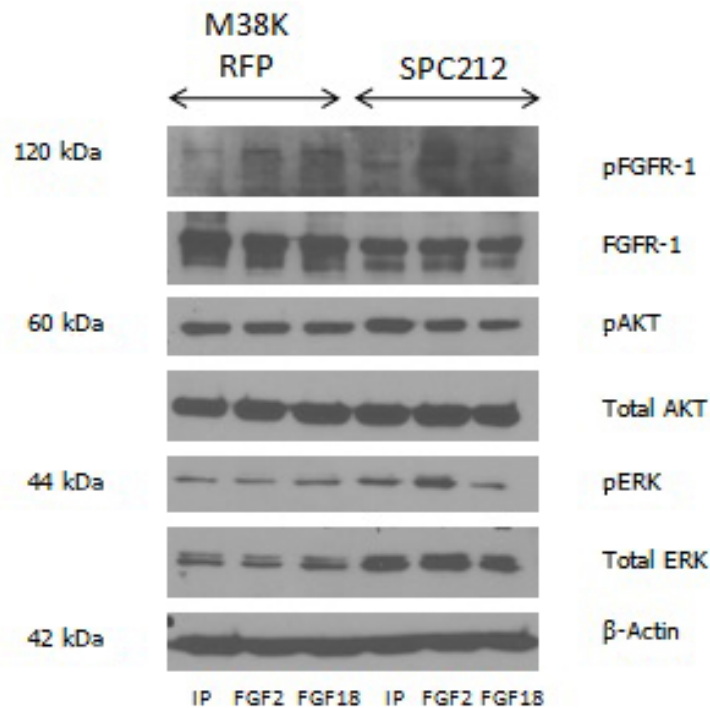
Figure 40: Only a slightly higher phosphorylation level of ERK in the SPC212 FGF2 cell line can be seen. However, more pFGFR-1 can be found in both cell lines overexpressing FGF2 or FGF18.

3.4 Epithelial-mesenchymal transition

3.4.1 EMT-markers

The treatment with FGF2 partially regulates the expression of known EMT-markers in the expected direction

Since FGF2 and EGF were described to induce EMT in cell lines like HT29 and DLD-1 [43], whole genome gene expression microarray data of FGF2- or EGF-treated M38K and SPC212 cell lines was checked for typical EMT-markers. It was found that E-cadherin, vimentin and ZEB1 are changing as expected, whereas MMP2, MMP9, snail and twist for instance did not show the expected regulation (see figure 41).

Gene name	EMT	M38K with FGF2
E–cadherin	⬇	✓
Vimentin	⬆	✓
ZEB1	⬆	✓
MMP2	⬆	✗
MMP9	⬆	✗
Snail	⬆	✗
Twist	⬆	✗

Figure 41: Change of classical EMT-markers in FGF2-treated M38K cells.

MMP1, MPP4, Smad7 and Smurf2 are clearly changed in our cells upon FGF2-treatment. These are genes which have been discussed as EMT-markers in some papers, but are not usually listed as classical EMT-markers (see figure 42 and the discussion).

Gene name	EMT	M38K with FGF2
MMP1	?	⬆
MPP4	?	⬆
Smad7	?	⬇
Smurf2	?	⬆

Figure 42: Change of other possible EMT-markers in FGF2-treated M38K cells.

Comparison of gene expression in FGF2- or EGF-treated MPM cell lines shows a distinctive regulation pattern in the biphasic cell lines undergoing morphology changes

For confirmation of the array data and further characterisation of the FGF2-induced changes in various cell lines qPCR with a set of 14 genes was performed. All genes were initially identified as differentially regulated upon treatment with FGF2 in M38K cells. The highest similarity to the regulation pattern of the FGF2-treated M38K cells was found in EGF-treated M38K. Expression levels of endocan (ESM1), integrin alpha 6 (ITGA6) and the transcription factor ETV4 were upregulated by treatment with FGF2 or EGF in M38K, whereas the levels of the TGF-β antagonist Smad7, the transcription factor GATA6 and the bradykinin receptor BDKRB2 were decreased. Some of these changes were also seen in the epithelioid MPM cell line VMC20 and in the biphasic SPC212 cell line, as well as in the transgenic M38K cells overexpressing FGF2. The biphasic MPM cell line SPC111 which does not show any morphology changes upon

FGF2 treatment also shows no increase in the expression levels of MMP1, MMP3, ESM1 and other genes, suggesting that these genes are connected to the EMT-like changes.

The changes in the gene expression were visualised in an unsupervised clustered heat map created with R. A downregulation of gene expression compared to untreated cells is shown in green (0-0.9), no changes upon treatment is shown in black (0.9-1.1) and an upregulation is shown in red (1.1<). No expression of a gene is shown in white (see figure 43).
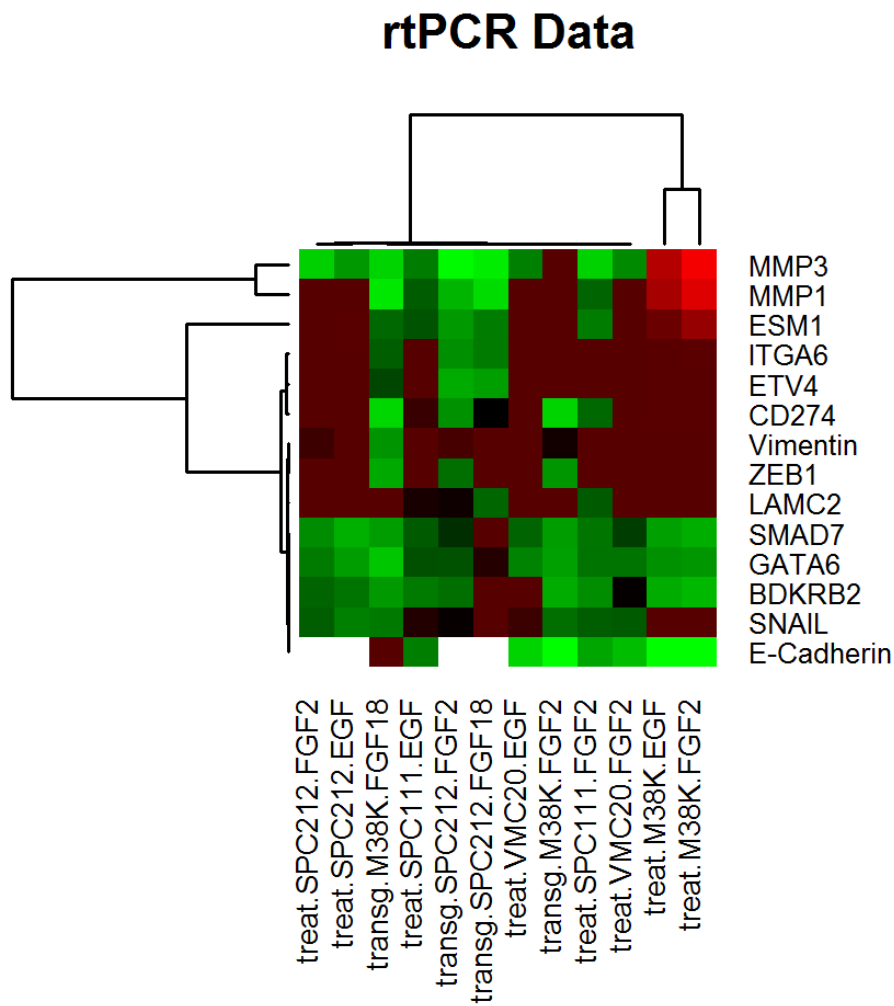
Figure 43: Heatmap of the qPCR results of FGF2- and EGF-treated cell lines.

4 Discussion

4.1 Cancer

Cancer is one of the greatest health problems in our world. When it comes to death rates, cancer carries off the gold medal in economically developed countries and secures the silver medal in developing countries. The most frequently diagnosed cancers in males are lung cancer, followed by prostate cancer in males, in females the leading cancer type is breast cancer [51]. It is, however, a disease which could be prevented to a considerable amount. Only 5 to 10% of all cancer cases are caused by hereditary genetic defects, the other 90 to 95% are due to exogenous factors which are to a large extend associated with lifestyle. This includes smoking, alcohol abuse, diet (especially red meat and fried food), obesity and lack of physical activity, infections (mainly in developing countries) and, as in the case of malignant pleural mesothelioma (MPM), exposure to environmental pollutants and carcinogenic agents [52].

Hanahan and Weinberg stated six hallmarks of cancer in 2000, and added two enabling characteristics and two emerging hallmarks in 2011, which I will only recapitulate shortly here. Genomic instability, which enables cells to accumulate gene defects, and sustaining inflammation which promotes tumor development are the enabling characteristics of cancer. In the case of MPM, asbestos fibers cause chronic inflammation in the lungs and DNA strand breaks in the cells. Resistance to cell death, evasion of growth suppressors, self-sufficiency in proliferative signaling and the ability to induce angiogenesis are four of the six hallmarks, which are carried out in MPM via expression and autocrine signaling of growth factors which promote survival, proliferation and, in the case of e.g fibroblast growth factor 2, angiogenesis. Replicative immortality and a invasive and migratory behavior are the last two typical characteristics of cancer cells stated by Hanahan and Weinberg. Two additional hallmarks, the emerging hallmarks as they called it, were added after more and more evidence emerged that tumor cells can avoid immune destruction and deregulate the cellular energetics [53].

Compared to lung or breast cancer, MPM is relatively rare, representing less than one percent of all cancer cases. Its main cause is inhalation of asbestos fibers. Asbestos is a silicate mineral which was widely used for construction after the second world war. After it was associated with various diseases of the respiratory tract in 1960, it was abandoned as building material in many western countries in the 1980s, but it was still used until 2005. Therefore, and because of

the long period of latency, an increase in new cases is expected in the next 10 to 20 years [54, 55].

The overall survival time after diagnosis is on average 10 months, due to the aggressiveness of the tumor and limited therapeutic options. The most successful chemotherapy regimen, pemetrexed in combination with cisplatin (both cytostatic drugs) can only prolong survival by about three months. Trimodality treatment including surgery, chemotherapy and radiation also shows only very modest results [56, 57]. Therefore new therapy methods are urgently needed. In various studies cytokines, their receptors and downstream signaling proteins were investigated as possible targets in MPM, for example inhibiting mammalian target of rapamycin (mTOR) with temsirolimus in combination with cisplatin [58] or inhibition of activin receptors, which impairs growth and migration of MPM cells *in vitro* [56]. Other targets that are used to combat several malignancies such as epidermal growth factor receptors (EGFR) or the inhibition of vascular endothelial growth factor (VEGF) with bevacizumab showed no significant results in clinical trials [59].

4.2 Fibroblast Growth Factors

As already described in the introduction, fibroblast growth factors (FGFs) are encoded by 22 genes in mammals and can be grouped in seven subfamilies. These growth factors act via binding to their high affinity receptors, the fibroblast growth factor receptor tyrosine kinases (FGFRs) [60]. For receptor-binding and signaling, heparan sulfate (HS) proteoglycans or (in the case of the endocrine FGFs) a mediator protein of the Klotho family is required [60, 61, 62]. FGFs and their receptors play various important roles in regulation of growth and differentiation of cells, wound healing, angiogenesis and embryonic development. Deregulation of the expression of FGFs or their receptors, or alteration in the kinase activity of the receptors, results in diverse pathologies including atherosclerosis, psoriasis, rheumatoid arthritis, and tumorigenesis [60, 63].

FGF2 in particular is known to have various important functions. It is known to regulate the expression of various genes involved in angiogenesis or metastasis, for example metalloproteinases or VEGF. FGF2 also suppresses the expression of E-cadherin in various cell types, which suggests a role in epithelial-mesenchymal transition (EMT) [64]. It mediates proliferation, differentiation and motility, and it was shown that it is one of the most important regulators of embryonic stem cell self-renewal and tumorigenesis in humans. There are five known molecular mass isoforms of FGF2, which are encoded by a single copy gene and alternatively translated [65].

It was recently shown that the tyrosine kinase inhibitor SU6668 which inhibits angiogenesis via blocking of the FGFR1, the VEGF Receptor 2 (VEGFR2) and the platelet-derived growth factor receptor β (PDGFRβ) is effective against sev-

eral malignancies in animal models. It also prolongs the survival of mice with MPM [66]. Additionally it was found, that MPM cell lines overexpress FGF2 and 18, as well as FGFR1. Inhibition of the kinase activity of FGFRs impairs the proliferation of MPM cells and synergizes with current chemotherapy [67]. In other human cancers, overexpression of FGFs and their receptors are already known to be involved in tumor progression and malignant behavior, for example in breast cancer [68], colorectal cancer [69] and prostate cancer [70].

The data of this thesis show that treatment of some biphasic MPM cell lines with FGF2 resulted in an increase of migration, as well as in significant cell scattering and morphology changes to a more fibroblastoid, spindle shaped morphology, under normal and also under serum-starved conditions. Other FGFs however (in particular FGF1, 5 and 18) did not induce such changes, suggesting a special role of FGF2. The described morphology changes require only a very short stimulus (one minute) and persist for about 72 h after the stimulus, indicating a very strong and fast signaling with very persistent effects. The changes in lateral migration behavior, induced via signaling via the FGFRs and the mitogen-activated protein kinase (MAPK) pathway can also be seen in retrovirally transduced cell lines overexpressing FGF2. FGF2 overexpressing M38K cells also form bigger spheroids in a low-attachment plate, suggesting an influence of FGF2 on the size of the tumor and the ability to grow anchor-independently.

Blocking the MAPK-pathway with the high affinity MEK-inhibitor Selumetinib results in a reduced proliferation and viability in most of the tested cell lines, suggesting a dependency on this pathway regarding growth and survival. Inhibiting the pathway with another MEK-inhibitor, UO126, also resulted in a decreased migration of the tested cell lines, which indicates also a role of this signaling-pathway in the aggressive behavior of the cells. Inhibiting the FGFR-1 with the selective inhibitor PD166866 (an ATP-competitive inhibitor which blocks the FGF2-induced transautophosphorylation of the kinase domains of the receptor [63]) prevents the morphology changes as well as phosphorylation of ERK in the downstream signaling cascade.

These findings regarding FGFs in MPM and the knowledge of FGF involvement in the malignancy of other human cancers suggests these growth factors and their high affinity receptors as potential targets in MPM therapy.

4.3 Epithelial-mesenchymal transition

Epithelial-mesenchymal transition (EMT) is a process best described for its role in embryonic development. During EMT epithelial cells lose their epithelial characteristics such as cell polarity and cell-cell adhesion, cells reorganize their cytoskeletal system and switch their gene expression patterns to become migratory, invasive, mesenchymal cells. These two characteristics already give us a hint that this process, usually tightly regulated during development, might be involved, but crucially deregulated, in tumor progression [71]. It was suggested that the reactivation of this process in an adult organism might be a response to

inflammation and an attempt to heal damaged tissue, two conditions that might be involved in cancer. Chronic inflammation, which is often involved in tumorigenesis could play a decisive role in the induction of this destructive EMT [72]. However, not all cells of a tumor undergo a complete EMT, nor is this process irreversible. To invade and migrate through the organism, cells need to break their cell-adhesions. Signals from the tumor microenvironment can induce EMT and cause at least some of the cells to shed their adhesions and other epithelial characteristics, and migrate to new destinations. When the signaling from the tumor microenvironment stops, cells can reverse the process of EMT and undergo mesenchymal-epithelial transition (MET) and settle in a new tissue, where they become generally known as metastases [71, 73]. EMT in cancer is not only associated with metastasis but also with cancer stem cells and resistance to chemo- and immunotherapy [74].

There are several well studied and characterized EMT markers for both epithelial and mesenchymal cells. The most prominent marker for epithelial cells is the calcium-dependend transmembrane glycoprotein E-cadherin, which is required for homophilic cell-cell adhesion. Expression and correct function of E-cadherin in cells is required to form stable adherens-junctions and to maintain the epithelial phenotype. Due to the fact that E-cadherin expression is frequently downregulated or even shut down completely in malignant carcinoma cells, E-cadherin is regarded as a tumor repressor gene, whose loss or malfunction is one of the crucial steps in tumor progression, invasion and metastasis [75].
It was already shown that E-cadherin expression levels are very low in many MPM cell lines [76]. A very low expression level of E-cadherin was also found in all of our MPM cell lines, as can be seen in figure 44. This heatmap shows the expression levels of several genes of untreated cells. The expression levels were calculated using the Ct-values obtained by qPCR. For normalization, the Ct-value of the housekeeping gene GAPDH was subtracted from the Ct-value of the measured gene, giving the ΔCt-value. Since the Ct-values are on a logarithmic scale with base 2, $2^{-\Delta Ct}$ gives a value for the absolute expression level, which was multiplied by 10^4. In figure 44 the expression levels from 0 to 5 are shown in black, 5 to 10 in blue, 10 to 100 in green and expression levels over 100 in yellow. The Met5a cell line is a mesothelial cell line, the MMO5 cell line is another biphasic cell line undergoing morphology changes upon FGF2 treatment (unpublished data).
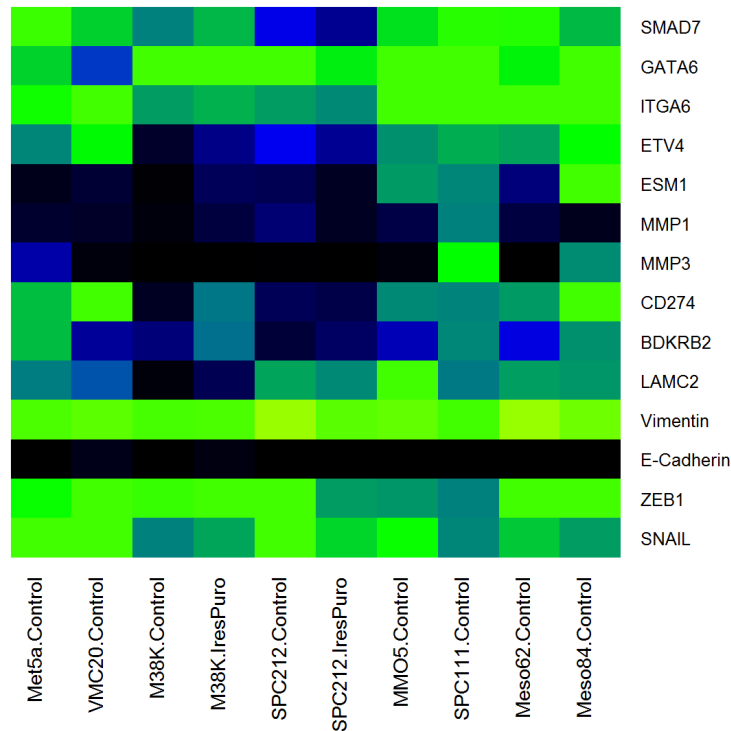
Figure 44: A low expression level of E-cadherin can be seen in all tested cell lines. Vimentin, snail1 and ZEB1 show high expression levels.

It can also be seen in this heatmap that our cell lines show a high expression level of the the three mesenchymal markers ZEB1 (zinc finger E-box-binding homeobox 1), vimentin and snail1.
Snail (snail1) is one member of a zinc-finger transcription factor superfamily and is involved in cell movement, usually during embryonic development but also in tumorigenesis where cells gain invasive and migratory properties [77]. The other members of this family, slug (snail2) and smuc (snail3), are involved in cell survival and differentiation. Snail1 is regulated via PI3K and Wnt signaling pathways, which govern the phosphorylation and nuclear localization of snail1, where it acts as a transcriptional repressor for e.g E-cadherin. EMT induced by snail involves therefore the downregulation of E-cadherin as well as of claudins and an upregulation of vimentin, ZEB1, the matrix metalloproteases MMP2 and MMP9 and other mesenchymal markers. Snail1 expression in cancer cells is usually associated with poor prognosis and metastases [74]. In MPM it was shown that a high expression level of snail1 results in poor prognosis and a shorter overall survival time of the patients. Snail1 and ZEB1 expressions are significantly higher in the more aggressive sarcomatoid and biphasic tumors compared to the epithelioid tumors. The high expression levels of snail1 also result in a low expression level of E-cadherin in the nonepithelioid tumors, which suggests an EMT in the nonepithelioid MPM subtypes [78]. In our tested cell lines the expression level of snail1 is very high and its expression is also increased upon

65

FGF2 stimulation in all tested cell line, except in the epithelioid cell line VMC20.

As mentioned before, the nuclear factor ZEB1 is another mesenchymal marker usually upregulated in sarcomatoid MPM cell lines. ZEB1 is known as an important factor in EMT and as a driver gene in the progression of epithelial cancers. It is known to be involved in tumor metastasis in breast and colon cancer and it is also expressed in most MPM cell lines. A transient knockdown of ZEB1 in MPM cell lines via siRNA was shown to reduce cell proliferation and to impair anchorage-dependent as well as anchorage-independent clonal growth [76]. ZEB1 is a transcriptional repressor of E-cadherin, a function which contributes to EMT and to a metastatic phenotype of many carcinomas. The repression of E-cadherin is carried out via an interaction between ZEB1 and the chromatin-remodelling protein BRG1 - blocking this interaction restores E-cadherin expression levels [79]. All of our tested cell lines have a high expression level of ZEB1 *a priori* and it is further upregulated upon stimulation with FGF2 and EGF.

Another mesenchymal marker upregulated by snail1 is vimentin, whose over-expression is as well associated with invasive growth, increased migration and a poor prognosis [74]. Vimentin is expressed in all mesenchymal cells as a component of the cytoskeleton, namely of the intermediate filament family. Since they are more stable than the other components of the cytoskeleton, intermediate filament proteins like vimentin are involved in maintaining the cellular integrity and in resisting mechanical cell stress. Due to its role in the cytoskeleton the over-expression of vimentin in tumor cells can be associated with increased invasive growth, as mentioned before. High expression levels of vimentin have been found in prostate and breast cancer, malignant melanoma, tumors in the gastrointestinal tract, the CNS and lung, as well as in other epithelial cancers. The exact role of vimentin in tumorigenesis and tumor progression is not known yet, however it is known to participate in various processes such as the regulation of heat shock genes, or as an indirect activator of Erk1/2 [80]. Like ZEB1 our tested cell lines have a high expression level of vimentin (due to their mesodermal origin), which is further upregulated upon FGF2- or EGF-treatment.

Twist, another mesenchymal marker upregulated in FGF2 treated M38K cells according to our array data was also found to be highly expressed in sarcomatoid tumors [81] but has to be further investigated in our cell lines yet.

One gene, which is no typical EMT marker but highly expressed in our cell lines and also upregulated upon FGF2 and EGF treatment is integrin-alpha 6 (ITGA6). Integrins have two functions in the cell: mediating interaction between cells and the ECM, and linking actin filaments to the cell membrane. They can also work as signal transducers, transmitting signals from outside the cell to the inside. Integrins can interact with RTKs via adaptor proteins to regulate cell survival, proliferation and differentiation on the one hand, and cell polarity, morphology, adhesions and migration on the other hand. Integrins were found to be

deregulated or malfunctioning in various tumor cells, probably contributing to multidrug resistance and a malignant phenotype [82]. ITGA6 is no EMT marker, but due to its roles in the regulation of the cytoskeleton and in RTK-signaling, it could be involved in the epithelioid-sarcomatoid transition we observed in our cell lines.

One could say that, since the normal mesothelial cells derive from the mesoderm, it is no wonder that MPM shows low levels of epithelial and high levels of mesenchymal markers [76]. On the other hand mesothelial cells form smooth cell layers with epithelial characteristics such as cell shape, tight junctions and the expression of epithelial cytokeratins [83]. Furthermore it was found, that during embryonic development pleural mesothelial cells can undergo EMT, sometimes referred to as mesothelial-mesenchymal transition (MMT), to migrate and form different mesenchymal structures in the heart, lung and gut. It was suggested that this process can be reactivated in adult organisms in response to lung-injury, which implies that mesothelial cells keep their plasticity also in adult organisms and change their phenotype depending on their environment [83, 84].
These findings underline the possibility of an EMT in MPM cells, potentially being responsible for the different histological subtypes. In addition, the great differences we found in the gene expression patterns, the morphology, the invasiveness, the migratory behavior and the overall aggressiveness between the different subtypes of MPM strongly suggest a drastic transformation from the less aggressive epithelioid to the sarcomatoid, more fibroblast-like type upon FGF2 treatment. It may not be a (complete) EMT but an epithelioid-sarcomatiod transition with underlying characteristics of an EMT.

4.4 Conclusion and outlook

Despite great progress in cancer research and therapy methods, MPM remains largely incurable yet. Long latency periods, diffuse and invasive growth along the pleura and resistance to current chemo- and radiotherapy contribute to a poor prognosis of this cancer. Although the use of asbestos, the main cause of MPM, is forbidden in many countries, the problem will not vanish. There are still countries in which asbestos is used for building, and also in countries where it is not used for new constructions anymore, it still remains in old buildings and the asbestos mines e.g in Australia are still considered as dangerous source of asbestos fibers. Therefore a better characterization of this cancer and - resulting from a better understanding - better therapy options are needed soon.

The changes in morphology, malignant behavior and expression patterns of biphasic and partially also epithelial cell lines upon treatment with FGF2, and the fact that FGF2 and FGFR1 were found to be highly expressed in MPM cell lines suggest a possible new therapy target. From our results we can say that the FGF-signaling axis contributes to the malignant behavior of this tumor as well

as to the survival of the tumor cells. Treatment with FGF2 increased the migration and anchorage independent growth of the cell lines, and inhibition of the involved pathways with specific inhibitors, for example the two MEK-inhibitors UO126 and Selumetinib, on the other hand results in a decrease of proliferation, migration and clonogenicity. Keeping also in mind that the sarcomatoid subtype of MPM is more aggressive and associated with worse prognosis but on the other side more sensitive to inhibition of the FGF signaling-pathways emphasizes the FGF signaling axis as a possibe target.

Further characterization of the histological subtypes and the transition from epithelioid to sarcomatoid behavior in some FGF2 stimulated biphasic cell lines with regards to the possibility of an underlying EMT might also be a good approach for a better understanding of this tumor. The sarcomatoid subtype seems to depend more on FGF2 signaling, and FGF2 stimulation results in the upregulation of typical mesenchymal markers in biphasic as well as epithelioid cell lines (despite the high basic transcript level). Since sarcomatoid tumors usually correlate with a worse prognosis and a shorter overall survival time, these findings could help to better understand this subtype and to find possible targets to at least lessen the aggressiveness of sarcomatoid tumors and prolong the survival time.

Since our findings strongly emphasize the importance of the FGF signaling axis in MPM cell lines regarding not only proliferation, migration and three dimensional growth but also in the formation of the different histological subtypes, this study will be continued with focus on the resemblance of the expression patterns of FGF2 stimulated nonsarcomatoid cell lines to those of sarcomatoid cell lines. Additionally the transgenic cell lines will be used to analyse the influence of FGF2 overexpression on the malignant behavior *in vivo*. The behavior of the cells upon stimulation with FGF2 or upon inhibition with various inhibitors of the FGF signaling axis will be further characterized. Especially in the sarcomatoid cell lines the dependence on the MAPK-pathway will be further analysed, regarding survival, proliferation and also the maintenance of the sarcomatoid morphology and the possibility of inducing MET in those cell lines.

5 Appendix

5.1 List of abbreviations

APES - Ammonium persulfate
ATP - Adenosine triphosphate
b2M - beta-2-Microtubulin
BDKRB2 - Bradykinin receptor B2
BMP2 - Bone morphogenetic protein
CV - Crystal violet
DAG - Diacylglycerol
DMEM - Dulbecco's Essential Eagle Medium
DNA - deoxyribonucleic acid
ECM - extracellular matrix
EDTA - Ethylenediaminetetraacetic acid
EGF - Epidermal growth factor
EGFR - Epidermal growth factor receptor
EGTA - Ethylene glycol tetraacetic acid
EMT - Epithelial-mesenchymal transition
EPP - Extrapleural pneumonectomy
Erk1/2 - Extracellular signal regulated kinases 1/2
ETV4 - ETS translocation variant 4
FCS - Fetal calf serum
FDU - FastDigest Unit
FGF - Fibroblast growth factor
FGF-BP - FGF-binding protein
FGFR - Fibroblast growth factor receptor
FHF - Fibroblast homologous factor
FRS2 - FGFR substrate 2
GAB1 - Grb2-associated binding protein
GAPDH - Glyceraldehyde 3-phosphate dehydrogenase
Grb2 - Growth factor receptor bound protein 2
GTP / GDP - Guanoside triphosphate / guanosine diphosphate
HCC - Hepatocellular carcinoma
HGF - Hepatocyte growth factor
HMGB-1 - High-mobility group protein B1
HS - Heparan sulfate
HSPG - Heparan sulfate proteoglycans
IP - IresPuro

ITGA6 - Integrin alpha 6
LAMC2 - Laminin subunit gamma-2
LB - Luria Bertani
LBII - Lysis buffer
M(P)M - Malignant (pleural) mesothelioma
MAPK - Mitogen activated protein kinase
MEK1 - Mitogen activated protein kinase 1
MEME - Minimum Essential Eagle Medium
MET - Mesenchymal-epithelial transition
MKP3 - MAPK phosphatase 3
MMP - Matrix metalloproteinase
MMT - Mesothelial-mesenchymal transition
MNP - MEME non-essential amino acids pyruvate
mTOR - Mammalian target of rapamycin
MTT - Dimethyl thiazolyl diphenyl tetrazolium salt
NFκB - Nuclear factor kappa-light-chain-enhancer of activated B-cells
PBS - Phosphate buffered saline
PCR - Polymerase chain reaction
PDGF - Platelet derived growth factor
PDGFR - Platelet derived growth factor receptor
PI3K - Phosphoinositide-3-kinase
PIP2 - Phosphatidylinositol-4,5-biphosphate
PIP3 - Phosphatidylinositol-3,4,5-triphosphate
PKB - Protein kinase B
PKC - Protein kinase C
PLCγ - Phospholipase C-gamma
PTB - Phosphotyrosin-binding domain
q(RT)PCR - Quantitative (real-time) polymerase chain reaction
RFP - Red fluorescent protein
RNA - Ribonucleic acid
RPMI - Roswell Park Memorial Institute
RTK - Receptor tyrosine kinase
SDS PAGE - Sodium dodecyl sulfate polyacrylamide gel electrophoresis
SH2 - Src homology 2
siRNA - small interfering RNA
SOS - Son of Sevenless
SPRy - Sprouty proteins
STAT - Signal transducer and activator of transcription
STET - NaCl/Tris/EDTA/TritonX-100
TBE - Tris/Borate/EDTA
TBS - Tris buffered saline
TE - Tris-EDTA
TEMED - N, N, N', N'-tetramethylenethylenediam
TNFα - Tumor necrosis factor alpha
VEGF - Vascular endothelial growth factor

VEGFR - Vascular endothelial growth factor receptor
ZEB1 - Zinc-finger E-box-binding homeobox 1

5.2 List of figures

5.3 List of tables

5.4 References

[1] R. M. Rudd, "Malignant mesothelioma," _Br Med Bull_, vol. **93**, pp. 105—-123, 2010.

[2] S. E. Mutsaers, "The mesothelial cell," _The International Journal of Biochemistry and Cell Biology_, vol. **36**, no. 1, pp. 9–16, 2004.

[3] M. G. Zauderer and L. M. Krug, "The evolution of multimodality therapy for malignant pleural mesothelioma," _Curr Treat Options Oncol._, vol. **12**, no. 2, pp. 163—-172, 2012.

[4] C. Bianchi and B. T., "Malignant mesothelioma: Global incidence and relationship with asbestos," _Industrial Health_, vol. **45**, no. 3, pp. 379–387, 2007.

[5] M. Muers, R. Stephens, _et al._, "Active symptom control with or without chemotherapy in the treatment of patients with malignant pleural mesothelioma (ms01): a multicentre randomised trial," _Lancet_, vol. **371**, no. 9625, pp. 1685–1694, 2008.

[6] M. Carbone, B. H. Ly, _et al._, "Malignant mesothelioma: Facts, myths and hypotheses," _J. Cell Physiol._, vol. **227**, no. 1, pp. 44–58, 2012.

[7] K. Donaldson, F. A. Murphy, _et al._, "Asbestos, carbon nanotubes and the pleural mesothelium: a review of the hypothesis regarding the role of long fibre retention in the parietal pleura, inflammation and mesothelioma," _Particle and Fibre Toxicology_, vol. **7**, no. 5, 2010.

[8] M. Carbone and H. Yang, "Targeting mechanisms of asbestos and erionite carcinogenesis in mesothelioma," _Clin Cancer Res._, vol. **18**, no. 3, pp. 598–604, 2012.

[9] D. W. Kufe, R. E. Pollock, _et al._, _Holland-Frei Cancer Medicine_. BC Decker, 6 ed., 2003. http://www.ncbi.nlm.nih.gov/books/NBK12354/.

[10] C. Casarsa, N. Bassani, *et al.*, "Epithelial-to-mesenchymal transition, cell polarity and stemness-associated features in malignant pleural mesothelioma," *Cancer Letters*, vol. **302**, pp. 136–143, 2011.

[11] M. R. Law, M. E. Hodson, and B. E. Heard, "Malignant mesothelioma of the pleura: relation between histological type and clinical behaviour," *Thorax*, vol. **37**, pp. 810–815, 1982.

[12] K. Schelch, "Evaluation of the fibroblast growth factor receptor axis as potential therapy target in malignant pleural mesothelioma," diploma thesis, University of Vienna, 2011.

[13] D. Sugarbaker and A. Wolf, "Surgery for malignant pleural mesothelioma," *Expert Rev. Resp. Med.*, vol. **4**, no. 3, pp. 363–372, 2010.

[14] J. Lindenmann, V. Matzi, *et al.*, "Multimodal therapy of malignant pleural mesothelioma: is the replacement of radical surgery imminent?," *Interactive CardioVascular and Thoracic Surgery*, vol. **16**, pp. 237—-243, 2013.

[15] L. Krug, H. Pass, *et al.*, "Multicenter phase ii trial of neoadjuvant pemetrexed plus cisplatin followed by extrapleural pneumonectomy and radiation for malignant pleural mesothelioma," *J Clin Oncol.*, vol. **27**, no. 18, pp. 3007–3013, 2009.

[16] R. Federico, F. Adolfo, *et al.*, "Phase ii trial of neoadjuvant pemetrexed plus cisplatin followed by surgery and radiation in the treatment of pleural mesothelioma.," *BMC Cancer*, vol. **13**, no. 22, 2013.

[17] M. de Perrot, R. Feld, *et al.*, "Trimodality therapy with induction chemotherapy followed by extrapleural pneumonectomy and adjuvant high-dose hemithoracic radiation for malignant pleural mesothelioma.," *J Clin Oncol.*, vol. **27**, no. 9, pp. 1413–1418, 2009.

[18] N. Itoh and D. Ornitz, "Fibroblast growth factors: from molecular evolution to roles in development, metabolism and disease," *J. Biochem.*, vol. **149**, no. 2, pp. 121–130, 2011.

[19] N. Turner and R. Grose, "Fibroblast growth factor signalling: from development to cancer," *Nat. Rev. Cancer*, vol. **10**, pp. 116–129, 2010.

[20] J. Wesche, K. Haglund, and M. Haugsten, "Fibroblast growth factors and their receptors in cancer," *Biochem. J.*, vol. **437**, pp. 199–213, 2011.

[21] D. Ornitz and H. Itoh, "Fibroblast growth factors," *Genome Biology*, vol. **2**, no. 3, pp. 3005.1—-3005.12, 2001.

[22] C. Heinzle, H. Sutterluty, *et al.*, "Targeting fibroblast-growth-factor-receptor-dependent signaling for cancer therapy," *Expert Opin Ther Targets*, vol. **15**, no. 7, pp. 829–846, 2011.

[23] B. Boilly, A. Vercoutter-Edouart, *et al.*, "Fgf signals for cell proliferation and migration through different pathways," *Cytokine and Growth Factor Reviews*, vol. **11**, no. 4, pp. 295–302, 2000.

[24] A. Aigner, M. Butscheid, *et al.*, "An fgf-binding protein (fgf-bp) exerts its biological function by parallel paracrine stimulation of tumor cell and endothelial cell proliferation through fgf-2 release," *Int. J. Cancer*, vol. **92**, pp. 510–517, 2001.

[25] T. Imamura, "Physiological functions and underlying mechanisms of fibroblast growth factor (fgf) family members: Recent findings and implications for their pharmacological application," *Biol. Pharm. Bull.*, vol. **37**, no. 7, pp. 1081–1089, 2014.

[26] A. Beenken and M. Mohammadi, "The fgf family: biology, pathophysiology and therapy," *Nat. Rev. Drug Discovery*, vol. **8**, no. 3, pp. 235–253, 2009.

[27] J. McCubrey, L. Steelman, *et al.*, "Roles of the raf/mek/erk pathway in cell growth, malignant transformation and drug resistance," *Biochimica et Biophysica Acta*, vol. **1773**, pp. 1263–1284, 2006.

[28] L. Steelman, W. Chappell, *et al.*, "Roles of the raf/mek/erk and pi3k/pten/akt/mtor pathways in controlling growth and sensitivity to therapy-implications for cancer and aging," *Aging*, vol. **3**, no. 3, pp. 192–222, 2011.

[29] K. Corbit, N. Trakul, *et al.*, "Activation of raf-1 signaling by protein kinase c through a mechanism involving raf kinase inhibitory protein," *J. Biol. Chem.*, vol. **278**, pp. 13061–13068, 2003.

[30] V. Knights and S. Cook, "De-regulated fgf receptors as therapeutic targets in cancer," *Pharmacology and Therapeutics*, vol. **125**, pp. 105–117, 2010.

[31] G. Liang, Z. Liu, *et al.*, "Anticancer molecules targeting fibroblast growth factor receptors," *Trends in Pharmacological Sciences*, vol. **33**, no. 10, pp. 531–541, 2012.

[32] T. Metzner, A. Bedeir, *et al.*, "Fibroblast growth factor receptors as therapeutic targets in human melanoma: Synergism with braf inhibition," *J. Invest. Dermatol.*, vol. **131**, no. 10, pp. 2087–2095, 2011.

[33] E. Sawey, M. Chanrion, *et al.*, "Identification of a therapeutic strategy targeting amplified fgf19 in liver cancer by oncogenomic screening," *Cancer Cell*, vol. **19**, no. 3, pp. 347–358, 2011.

[34] G. Sonvilla, S. Allerstorfer, *et al.*, "Fibroblast growth factor receptor 3-iiic mediates colorectal cancer growth and migration," *Br. J. Cancer*, vol. **102**, no. 7, pp. 1145–1156, 2010.

[35] C. L'Hôte and M. Knowles, "Cell responses to fgfr3 signalling: growth, differentiation and apoptosis," *Experimental cell research*, vol. **304**, no. 2, pp. 417–431, 2005.

[36] H. Fischer, N. Taylor, *et al.*, "Fibroblast growth factor receptor-mediated signals contribute to the malignant phenotype of non-small cell lung cancer cells: therapeutic implications and synergism with epidermal growth factor receptor inhibition," *Mol. Cancer Ther.*, vol. **7**, pp. 3408–3419, 2008.

[37] J. Dey, F. Bianchi, *et al.*, "Targeting fibroblast growth factor receptors blocks pi3k/akt signaling, induces apoptosis, and impairs mammary tumor outgrowth and metastasis," *Cancer Res.*, vol. **70**, no. 10, pp. 4151–4162, 2010.

[38] J. Lim and J. Thiery, "Epithelial-mesenchymal transitions: insights from development," *Development*, vol. **139**, no. 19, pp. 3471–3486, 2012.

[39] D. Radisky, "Epithelial-mesenchymal transition," *Journal of Cell Science*, vol. **118**, pp. 4325–4326, 2005.

[40] A. Fassina, R. Cappellesso, *et al.*, "Epithelial-mesenchymal transition in malignant mesothelioma," *Modern Pathology*, vol. **25**, pp. 86–99, 2012.

[41] R. Kalluri and R. Weinberg, "The basics of epithelial-mesenchymal transition," *J. Clin. Invest.*, vol. **119**, no. 6, pp. 1420–1428, 2009.

[42] J. Taube, J. Herschkowitz, *et al.*, "Core epithelial-to-mesenchymal transition interactome gene-expression signature is associated with claudin-low and metaplastic breast cancer subtypes," *PNAS*, vol. **107**, no. 35, pp. 15449–15454, 2010.

[43] K. Sakuma, M. Aoki, and R. Kannagi, "Transcription factors c-myc and cdx2 mediate e-selectin ligand expression in colon cancer cells undergoing egf/bfgf-induced epithelial-mesenchymal transition," *PNAS*, vol. **109**, no. 20, pp. 7776–7781, 2012.

[44] B. Greber, H. Lehrach, and J. Adjaye, "Fibroblast growth factor 2 modulates transforming growth factor beta signaling in mouse embryonic fibroblasts and human esc (hesc) to support hesc self-renewal," *Stem Cells*, vol. **25**, no. 2, pp. 455–464, 2007.

[45] S. Grotegut, D. von Schweinitz, *et al.*, "Hepatocyte growth factor induces cell scattering through mapk/egr-1-mediated upregulation of snail," *The EMBO Journal*, vol. **25**, no. 15, pp. 3534–3545, 2006.

[46] T. Nagai, T. Arao, *et al.*, "Sorafenib inhibits the hepatocyte growth factor-mediated epithelial mesenchymal transition in hepatocellular carcinoma," *Mol Cancer Ther*, vol. **10**, no. 1, pp. 169–177, 2011.

[47] B. Alberts, A. Johnson, *et al.*, *Molecular Biology of the Cell*. Garland Science, 5 ed., 2008.

[48] R. Verma and C. Hansch, "Matrix metalloproteinases: Chemical-biological functions and (q)sars," *Bioorganic and Medicinal Chemistry*, vol. **15**, no. 6, pp. 2223–2268, 2007.

[49] H. Nagase and J. Woessner Jr., "Matrix metalloproteinases," *J. Biol. Chem.*, vol. **274**, no. 31, pp. 21491–21494, 1999.

[50] A. Abolhassani, G. Riazi, *et al.*, "Fgf10: Epithelial mesenchymal transition and invasion in breast cancer cell lines," *J. Cancer*, vol. **5**, no. 7, pp. 537–547, 2014.

[51] A. Jemal, F. Bray, *et al.*, "Global cancer statistics," *CA Cancer J. Clin.*, vol. **61**, pp. 69–90, 2011.

[52] P. Anand, A. Kunnumakara, *et al.*, "Cancer is a preventable disease that requires major lifestyle changes," *Pharmaceutical Research*, vol. **25**, no. 9, pp. 2097–2116, 2008.

[53] D. Hanahan and R. Weinberg, "Hallmarks of cancer: the next generation.," *Cell*, vol. **144**, no. 5, pp. 646–674, 2011.

[54] T. Ploenes, T. Osei-Agyemang, *et al.*, "Malignant pleural mesothelioma," *Dtsch. Med. Wochenschr.*, vol. **137**, no. 10, pp. 481–486, 2012.

[55] A. Moore, R. Parker, and J. Wiggins, "Malignant mesothelioma," *Orphanet Journal of Rare Diseases*, vol. **3**, no. 34, 2008.

[56] M. Hoda, J. Münzker, *et al.*, "Suppression of activin a signals inhibits growth of malignant pleural mesothelioma cells," *British Journal of Cancer*, vol. **107**, pp. 1978–1986, 2012.

[57] N. Vogelzang, J. J. Rusthoven, *et al.*, "Phase iii study of pemetrexed in combination with cisplatin versus cisplatin alone in patients with malignant pleural mesothelioma," *J. Clin. Oncol.*, vol. **21**, no. 14, pp. 2636–2644, 2003.

[58] M. Moriya, T. Yamada, *et al.*, "Antitumor effect and antiangiogenic potential of the mtor inhibitor temsirolimus against malignant pleural mesothelioma," *Oncology Reports*, vol. **31**, no. 3, pp. 1109–1115, 2014.

[59] R. Kelly, E. Sharon, and R. Hassan, "Chemotherapy and targeted therapies for unresectable malignant mesothelioma," *Lung Cancer*, vol. **73**, no. 3, pp. 256–263, 2011.

[60] X. Zhang, O. Ibrahimi, *et al.*, "Receptor specificity of the fibroblast growth factor family," *J. Biol. Chem.*, vol. **281**, no. 23, pp. 15694–15700, 2006.

[61] M. Potthoff, S. Kliewer, *et al.*, "Endocrine fibroblast growth factors 15/19 and 21: from feast to famine," *Genes Dev.*, vol. **26**, no. 4, pp. 312–324, 2012.

[62] S. Fukumoto, "Receptor specificity of the fibroblast growth factor family," *Endocrine Journal*, vol. **55**, no. 1, pp. 23–31, 2008.

[63] R. Panek and G. Lu, "In vitro biological characterization and antiangiogenic effects of pd 166866, a selective inhibitor of the fgf-1 receptor tyrosine kinase," *The Journal of Pharmacology and Experimental Therapeutics*, vol. **286**, no. 1, pp. 569–577, 1998.

[64] M. Lau, W. So, and P. Leung, "Fibroblast growth factor 2 induces e-cadherin down-regulation via pi3k/akt/mtor and mapk/erk signaling in ovarian cancer cells," *PLoS One*, vol. **8**, no. 3, 2013.

[65] P. Dvorak, D. Dvorakova, and A. Hampl, "Fibroblast growth factor signaling in embryonic and cancer stem cells," *FEBS Letters*, vol. **580**, pp. 2869–2874, 2006.

[66] T. Van, M. Hanibuchi, *et al.*, "Su6668, a multiple tyrosine kinase inhibitor, inhibits progression of human malignant pleural mesothelioma in an orthotopic model," *Respirology*, vol. **17**, pp. 984–990, 2012.

[67] K. Schelch, M. Hoda, *et al.*, "Fgf receptor inhibition is active against mesothelioma and synergizes with radio- and chemotherapy.," *Am J Respir Crit Care Med.*, 2014.

[68] A. Letessier, F. Sircoulomb, *et al.*, "Frequency, prognostic impact, and subtype association of 8p12, 8q24, 11q13, 12p13, 17q12, and 20q13 amplifications in breast cancers," *BMC Cancer*, vol. **6**, no. 245, 2006.

[69] N. Jibiki, N. Saito, *et al.*, "Clinical significance of fibroblast growth factor (fgf) expression in colorectal cancer.," *Int. Surg.*, vol. **99**, no. 5, pp. 493–499, 2014.

[70] T. Murphy, S. Darby, *et al.*, "Evidence for distinct alterations in the fgf axis in prostate cancer progression to an aggressive clinical phenotype.," *J. Pathol.*, vol. **220**, no. 4, pp. 452–460, 2010.

[71] M. Klymkowsky and P. Savagner, "Epithelial-mesenchymal transition - a cancer researcher's conceptual friend and foe," *The American Journal of Pathology*, vol. **174**, no. 5, pp. 1588–1593, 2009.

[72] J. López-Novoa and M. Nieto, "Inflammation and emt: an alliance towards organ fibrosis and cancer progression," *EMBO Mol. Med.*, vol. **1**, no. 6-7, pp. 303–314, 2009.

[73] C. Dong, Y. Wu, *et al.*, "G9a interacts with snail and is critical for snail-mediated e-cadherin repression in human breast cancer," *J. Clin. Invest.*, vol. **122**, no. 4, pp. 1469–1486, 2012.

[74] S. Kaufhold and B. Bonavida, "Central role of snail1 in the regulation of emt and resistance in cancer: a target for therapeutic intervention," *Journal of Experimental and Clinical Cancer Research*, vol. **33**, no. 62, 2014.

[75] N. Pećina-Šlaus, "Tumor suppressor gene e-cadherin and its role in normal and malignant cells," *Cancer Cell Int.*, vol. **3**, no. 17, 2003.

[76] M. Horio, M. Sato, *et al.*, "Transient but not stable zeb1 knockdown dramatically inhibits growth of malignant pleural mesothelioma cells," *Ann. Surg. Oncol.*, vol. **19**, pp. 634–645, 2012.

[77] M. Nieto, "The snail superfamily of zinc-finger transcription factors.," *Nat. Rev. Mol. Cell Biol.*, vol. **3**, no. 3, pp. 155–166, 2002.

[78] M. Kobayashi, C. Huang, *et al.*, "Snail expression is associated with a poor prognosis in malignant pleural mesotheliomas," *Ann. Thorac. Surg.*, vol. **95**, pp. 1181–1188, 2013.

[79] E. Sanchéz-Tilló, A. Lázaro, *et al.*, "Zeb1 represses e-cadherin and induces an emt by recruiting the swi/snf chromatin-remodeling protein brg1.," *Oncogene*, vol. **29**, no. 24, pp. 3490–3500, 2010.

[80] A. Satelli and S. Li, "Vimentin as a potential molecular target in cancer therapy or vimentin, an overview and its potential as a molecular target for cancer therapy," *Cell Mol. Life Sci.*, vol. **68**, no. 18, pp. 3033–3046, 2011.

[81] T. Iwanami, H. Uramoto, *et al.*, "Clinical significance of epithelial-mesenchymal transition-associated markers in malignant pleural mesothelioma.," *Oncology*, vol. **82**, no. 2, pp. 109–116, 2014.

[82] S. Hehlgans, M. Haase, and N. Cordes, "Signalling via integrins: Implications for cell survival and anticancer strategies," *BBA - Reviews on Cancer*, vol. **1775**, no. 1, pp. 163–180, 2007.

[83] H. Batra and V. Antony, "The pleural mesothelium in development and disease," *Frontiers in Physiology*, vol. **5**, no. 284, 2014.

[84] S. Herrick and S. Mutsaers, "Mesothelial progenitor cells and their potential in tissue engineering," *The International Journal of Biochemistry and Cell Biology*, vol. **36**, no. 4, pp. 621–642, 2004.

Zusammenfassung

Das maligne Pleuramesotheliom (MPM) ist eine relativ seltene, sehr aggressive Krebsart, die häufig durch Inhalation von Asbestfasern ausgelöst wird. Da derzeitige Therapiemethoden schlecht anschlagen, werden neue Therapiemöglichkeiten gebraucht. Rezeptor-Tyrosinkinasen (RTKs), speziell Fibroblasten-Wachstumsfaktor-Rezeptoren (fibroblast growth factor receptors, FGFR) spielen eine Rolle in der Entwicklung und im Voranschreiten von Krebs, daher könnten sie als Angriffspunkte bei einer Therapie genutzt werden. Epitheliale-mesenchymale Transition (EMT) ist ein häufig beobachtetes Phänomen in der Entwicklung von Krebs, bei dem epitheliale Zellen ihre Zell-Zell-Kontakte verlieren und ihr Migrations- und Invasionspotential steigern.

Ziele: Das Ziel dieser Arbeit war, den Einfluss verschiedener Wachstumsfaktoren und (RTK-)Inhibitoren auf MPM Zelllinien im Bezug auf Änderungen der Morphologie, der Migration und der Proliferation zu analysieren. Mein Fokus lag insbesondere auf dem Fibroblasten-Wachstumsfaktor 2 (fibroblast growth factor 2, FGF2).

Methoden: Die Zelllinien wurden mit verschiedenen Wachstumsfaktoren und/ oder Inhibitoren behandelt. Aufgetretene Morphologieänderungen wurden unter dem Mikroskop beobachtet beziehungsweise für weitere Charakterisierung fotographiert. Zur Charakterisierung von Proliferation und Migration wurden verschiedene *in vitro* Tests durchgeführt. Veränderungen auf Protein- und Transkriptionsebene wurden durch Western blots, Microarrays und qPCR analysiert. Weiters wurden durch retrovirale Transfektion transgene Zelllinien hergestellt und charakterisiert.

Ergebnisse: FGF2-Behandlung induzierte Morphologieänderungen und eine Steigerung der Migration in einigen MPM Zelllinien. Diese Änderungen werden durch Signaltransduktion über den MAPK-Signalweg vermittelt. Expressionsanalysen haben gezeigt, dass die Expressionslevel einiger typischer EMT-Marker wie zum Beispiel E-Cadherin, Vimentin und Zeb1 in FGF2 behandelten Zellen entsprechend einer EMT reguliert sind. Einige zusätzliche Transkripte wurden als verändert identifiziert und könnten ebenfalls eine Rolle bei den beobachteten funktionellen und morphologischen Veränderungen spielen.

Schlussfolgerung: Diese Daten zeigen, dass FGF2 wichtige Veränderungen sowohl in der Genxpression als auch im Verhalten der Zellen induziert. Dies deutet darauf hin, dass FGF2 eine wichtige treibende Rolle in der Agressivität und möglicherweise in der EMT dieser Krebsart spielt.

Abstract

Malignant pleural mesothelioma (MPM) is a relatively rare, highly aggressive tumor, which is often a consequence of exposure to asbestos. Its resistance to current chemo- and radiotherapy makes the search for new therapeutic approaches necessary. Receptor tyrosine kinases (RTKs), specifically the fibroblast growth factor receptors (FGFRs), are known to play an important role in the development as well as in the progression of cancer, therefore FGFRs and their ligands are suggested as additional therapeutic targets in various cancers. Epithelial to mesenchymal transition (EMT) is frequently observed in the progression of cancer, whereby epithelial cells lose their cell-cell contacts and gain migratory as well as invasive abilities.

Objectives: The aim of this study was to investigate the influence of various growth factors and inhibitors of RTKs or their downstream targets on MPM cell lines regarding morphology and proliferation. In detail, I focussed on the effects of FGF2 treatment or overexpression on migration, proliferation, spheriod formation, as well as EMT-like behavior and expression changes.

Methods: Cells were treated with various growth factors and/or inhibitors to analyse their effects, regarding morphology and migration as well as EMT-like changes. Changes on the protein and the transcriptional level upon treatment were investigated using immunoblotting, microarray analysis and qPCR, respectively. Additionally transgenic cell lines were established using retroviral transfection. For the characterization of the migration behavior, growth and proliferation of the cells overexpressing FGF2, several *in vitro* assays were performed.

Results: Immunoblotting and treatment with various inhibitors showed that FGF2 induces the observed changes by signaling via the MAPK-pathway. Migration assays showed that treatment with FGF2 as well as stable overexpression of FGF2 increases cell migration. Expression analysis showed that some typical EMT markers like E-cadherin, vimentin and ZEB1 are regulated as expected for EMT upon treatment with FGF2. In addition, several other transcripts were found to be distinctively regulated, suggesting an involvement in the behavioral and morphological changes.

Conclusions: These data show that FGF2 induces crucial changes in gene expression as well as in the behavior of the cells, suggesting that it may be an important factor driving EMT in MPM cells, resulting in the high aggressiveness of this tumor.

CURRICULUM VITAE
Christina Maria Wagner

Education

Since **winter semester 2013**: Master study of <u>Molecular Biology</u> (focus on molecular medicine) at the University of Vienna

Winter semester 2009 – summer semester 2013: Undergraduate study of <u>Biology</u> (focus on molecular biology) at the University of Vienna

Winter semester 2007 – summer semester 2011: Undergraduate study of <u>Japanese Studies</u> at the University of Vienna

2007: Graduation - <u>school certificate examination</u> at Bundesrealgymnasium 18, Vienna

Professional Experience

01/2013 – 09/2014: Institute of Cancer Research (ICR), Department of Medicine I, Medical University of Vienna (Group M. Grusch) - <u>Diploma thesis</u> "Growth Factor-Induced Epithelioid-Sarcomatoid Transition in Malignant Pleural Mesothelioma Cells?"

Teaching Activities

02/2014: Supervision of an undergraduate student's internship

01/2014: PhD seminar „Molecular Cloning", supervision of lab work

01/2012 – 01/2013: Tutor for the lecture "Allgemeine und organische Chemie für Biologen" at the University of Vienna

Publications

"FGF Receptor Inhibition is Active Against Mesothelioma and Synergizes with Radio- and Chemotherapy."

K. Schelch, MA. Hoda, T. Klikovits, J. Münzker, B. Ghanim, <u>C. Wagner,</u> et al

Am J Respir Crit Care Med. – October 2014

PMID: 25188816

Poster and Oral Presentations

11/2014

"Exploring Cell Plasticity in Malignant Pleural Mesothelioma" (Poster presentation)

C. Wagner, K. Schelch, MA. Hoda, T. Klikovits, G. Reid, W. Berger, B. Hegedus, B. Dome, W. Klepetko and M. Grusch

14th Central European Lung Cancer Conference, Vienna, Austria

10/2014

"Cell models to study epithelial mesenchymal transition in malignant pleural mesothelioma"

C. Wagner, K. Schelch, MA. Hoda, T. Klikovits et al

12th International Mesothelioma Interest Group (IMIG) Conference, Cape Town, South Africa

06/2014

"FGF2 Induces EMT-like Behaviour and Expression Changes in Malignant Pleural Mesothelioma Cells" (Poster presentation)

C. Wagner, K. Schelch, B. Peter-Vörösmarty, MA. Hoda, B. Hegedus, B. Dome, W. Berger and M. Grusch

10th YSA-PhD-Symposium, Medical University Vienna, Austria

10/2013

"An inducible transition cell model reflecting epithelioid versus sarcomatoid differentiation of Malignant Pleural Mesothelioma"

K. Schelch, C. Wagner, MA. Hoda, B. Hegedus, B. Dome, W. Berger, W. Klepetko and M. Grusch

15th World Conference of Lung Cancer, IASLC Sydney, Australia

06/2013

"Fibroblast Growth Factor Signaling in Malignant Pleural Mesothelioma: Regulation, Oncogenic Functions and Therapeutic Options"

K. Schelch, M. A. Hoda, C. Wagner, B. Hegedus, B. Dome, W. Berger, W. Klepetko, and M. Grusch

9th YSA-PhD-Symposium, Medical University Vienna, Austria